Contrib Mineral Petrol (2005) 150: 230–249
DOI 10.1007/s00410-005-0019-6

ORIGINAL PAPER

A. I. S. Kemp · M. J. Whitehouse · C. J. Hawkesworth
M. K. Alarcon

A zircon U-Pb study of metaluminous (I-type) granites of the Lachlan Fold Belt, southeastern Australia: implications for the high/low temperature classification and magma differentiation processes

Received: 8 October 2004 / Accepted: 4 July 2005 / Published online: 12 August 2005

Abstract Following seminal studies in the Lachlan Fold Belt (southeastern Australia), it has become almost axiomatic that metaluminous granites derive from *infracrustal* precursors, whereas strongly peraluminous plutons have metasedimentary or *supracrustal* sources, as reflected in the I- and S-type designation. Recently, zircon saturation thermometry has been used to further subdivide I-type granites into high- and low-temperature categories. That low-temperature I-type granites evolved by restite separation from magmas generated in the zircon stability field is implicit in this classification. To explore this hypothesis, we report an ion microprobe U-Pb (zircon) study into three hallmark 'low-temperature' Lachlan Fold Belt I-type suites. The combined patterns of zircon age inheritance and bulk rock Zr trends suggest that each suite formed from magmas that were initially zircon-undersaturated, and that fractional crystallisation, not restite unmixing, was the dominant differentiation process. The low temperature status presently applied to these rocks cannot therefore be justified. The inherited zircons in these I-type granites reflect melting and assimilation of metasedimentary rock, and testify to a supracrustal source component.

Electronic Supplementary Material Supplementary material is available for this article at http://dx.doi.org/10.1007/s00410-005-0019-6

Communicated by B. Collins

A. I. S. Kemp (✉) · C. J. Hawkesworth
Department of Earth Sciences, University of Bristol, Bristol B58 IRJ, UK
E-mail: tony.kemp@geo.sc.niigata-u.ac.jp

M. J. Whitehouse
Swedish Museum of Natural History, Box 50007, 10405 Stockholm, Sweden

M. K. Alarcon
31 Ashburton Circuit, Kaleen, ACT, 2617, Australia

Present address: A. I. S. Kemp
Department of Geology, Faculty of Science, Niigata University, 2-8050 Ikarashi, Niigata, 950-2181, Japan

Introduction

The temperatures at which silicic magmas are generated, and whether these depart the source in essentially liquid state or as partially crystalline 'mushes' are key questions in granite petrogenesis, and hence for models of the chemical evolution of the continental crust. Such issues have proved to be difficult to resolve, impeding our understanding of (1) the extent to which granites incorporate contributions from mantle and crustal components, (2) the conditions of melting and the nature of the heat sources, (3) the mechanisms of magma extraction, and (4) the processes that control the compositional diversity of granitic rocks.

Nowhere have these issues been more exhaustively debated than in the Palaeozoic Lachlan Fold Belt, a classic granite province in southeastern Australia. Despite nearly three decades of intensive study, the relative roles of intrinsically high-temperature differentiation processes, like fractional crystallisation or magma mixing, versus the separation of restite from relatively low-temperature melt, remain keenly contested (e.g. Collins 1998, 1999 versus Chappell et al. 1999, 2000). Recent studies (Chappell et al. 1998, 2000; and see also Miller et al. 2003) have sought to clarify these issues by using the granitic accessory mineral zircon, specifically by coupling the presence or absence of pre-magmatic 'inherited' zircon cores with zircon saturation thermometry (Watson and Harrison 1983). This approach has led to the notion of 'low'- and 'high'-temperature granites (Chappell et al. 1998). The low-temperature granites are those that contain abundant inherited zircon, and they are inferred to have formed at temperatures below that required for the complete dissolution of this mineral in the protolith. In this circumstance, zircon saturation thermometry (T_{Zr}), which yields the upper temperature limit at which a zircon crystal could survive in a melt *having the composition of the bulk rock*, potentially constrains the maximum temperature of granitic magma generation (Miller et al. 2003). Conversely, high-temperature granites lack inherited zircon. Instead, the zircons present have crystallised from hot, essentially liquid magmas that were initially undersaturated in zircon. For these rocks, T_{Zr} provides a minimum temperature estimate only.

Intriguingly, for the hornblende-bearing granites of the LFB that contain inherited zircon, T_{Zr} consistently falls below 800°C, even for tonalites that resemble the subduction-related plutons of the circum-Pacific Cordilleras (Chappell et al. 2001). These temperatures are much lower than the liquidus temperatures of such compositions, established experimentally to exceed 950°C (Piwinski and Wyllie 1968; Stern et al. 1975; Huang and Wyllie 1986). This observation has fuelled the restite model, which asserts that rather than complete melts, the granitic magmas were replete with residual source material, and evolved by the differential separation of this refractory crystal cargo from a low-temperature felsic melt, producing straight line chemical variations. In this model, the necessity for thermal extremes in the crust during orogenesis is obviated, along with the geotectonic scenarios invoked to obtain these conditions (e.g. Petford and Gallagher 2001).

To explore the implications of zircon saturation systematics for silicic magma genesis, and the validity of the high/low-temperature scheme in general, this paper reports an ion microprobe U-Pb study of zircons from three metaluminous granitic suites of the LFB. The zircon populations and chemical trends suggest that the low T_{Zr} for the most mafic rocks of each suite reflect

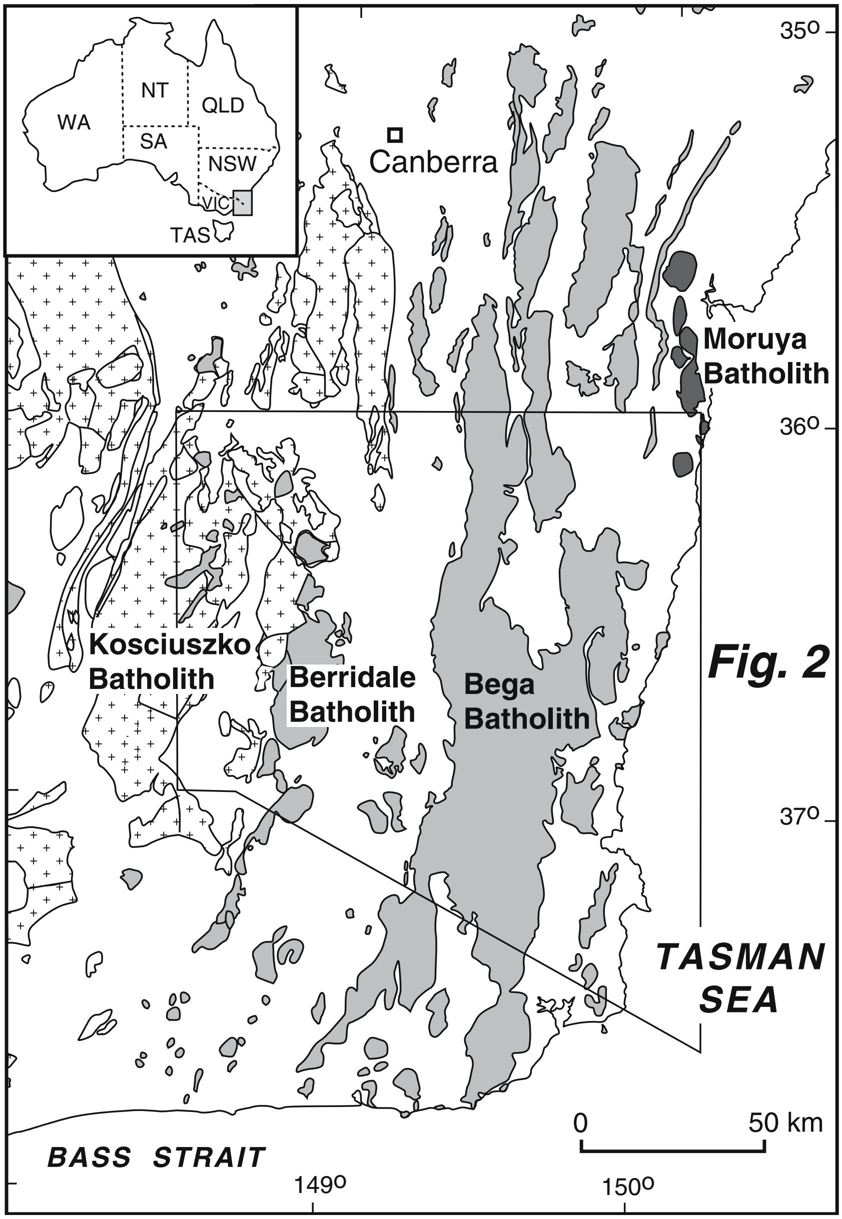

Fig. 1 Simplified geological map of the Lachlan Fold Belt in eastern Australia showing the location of the granitic batholiths referred to in the text and the distribution of the 'I-type' (*shaded*) and 'S-type' (*crosses*) intrusions. The volumetrically minor gabbroic bodies and A-type granites are also *shaded*. The locality of Fig. 2 is indicated

zircon saturation late within the crystallisation sequence of an initially high-temperature magma, consistent with compositional control by fractional crystallisation. Rather than indicating magma generation in the zircon stability field, the inherited zircons of each suite are interpreted as xenocrysts, in some cases metastably preserved, that manifest a metasedimentary component within the LFB metaluminous granites.

Geological background

The LFB is part of a 3,600-km long orogenic system that developed along the eastern Gondwana continental margin from the Early Ordovician to Devonian (see Gray 1997). It has two main components, a monotonous sequence of Ordovician to Silurian turbidites, and a large volume of granitic and felsic volcanic units. The turbidites were subject to episodic deformation, regional metamorphism (mostly greenschist facies) and massive igneous intrusion from ~450–340 Ma (Gray and Foster 1997).

The early, seminal granitic studies were conducted in the eastern LFB, where the dichotomy between the hornblende-bearing (metaluminous to weakly peraluminous) and cordierite-bearing (strongly peraluminous) granites was first recognised and the restite model formulated (Chappell and White 1974; White and Chappell 1977). The key conclusion of these studies is that the contrasting mineralogy and geochemistry of the two granitic types reflects derivation from disparate protoliths. The cordierite granites are presumed to have metasedimentary sources, which complies with most field, experimental and chemical data (Clemens 2003). On the other hand, the hornblende granites are assigned a meta-igneous or infracrustal precursor that has not experienced a weathering cycle, such as an accreted mafic underplate (Chappell and Stephens 1988). This notion has engendered the S- and I-type paradigm that pervades granite literature. However, isotopic evidence points to the involvement of both sedimentary materials and juvenile mantle-derived liquids in hornblende granite genesis (Gray 1984; Keay et al. 1997), which challenges the I-type status and has different implications for continental crustal evolution (Kemp and Hawkesworth 2003).

Granitic rocks of the eastern LFB comprise vast, meridionally trending batholiths, including from west to east, the Kosciuszko, Berridale and Bega Batholiths (Fig. 1). The Bega Batholith comprises almost exclusively hornblende granites but it is compositionally asymmetric, such that rocks become systematically more sodic, richer in Sr and isotopically primitive towards the continental margin (Chappell et al. 1991). Plutons within these batholiths are grouped into suites and supersuites, where rocks of a given suite define coherent chemical trends and are assumed to be consanguineous. However, understanding the causes of inter- and intra-suite compositional variation continues to be challenging. Zircon studies are potentially invaluable in pursuit of this aim, especially in unravelling the competing effects of differing source materials versus magma generation processes.

Previous U-Pb zircon studies and their implications

The published U-Pb zircon data from metaluminous granites of the eastern LFB is limited to plutons of the Bega and Kosciuszko batholiths. Hoskin (2000) and Hoskin et al. (2000) document the morphologies and age populations, respectively, of zircons within the c. 410 Ma Boggy Plain Pluton of the Kosciuszko Batholith. This body is concentrically zoned from marginal gabbro and diorite, through granodiorite and monzogranite, to an aplitic core (Wyborn et al. 2001). Textural and geochemical evidence suggests that the lower silica, pyroxene-rich rocks are cumulates formed by fractional crystallisation of a hot (~1,100°C) aphyric parental magma (Wyborn et al. 2001). Zirconium abundances rise from low concentrations in the diorites, suggesting initial Zr undersaturation, until a sharp downward inflection at ~66% SiO_2, which signals the onset of zircon crystallisation from the evolving liquid. For this reason, the Boggy Plain pluton is a classic 'high-temperature' type (Chappell et al. 1998, 2000). Inherited zircons occur in the felsic zones of the pluton, and are interpreted as xenocrysts derived by assimilation of sedimentary wall-rocks by the zircon-saturated residual melt (Hoskin et al. 2000). However, older cores are also encountered in every zircon analysed in a granodiorite of distinctly lower silica content than the inferred zircon saturation point (sample BP16, 62.3% SiO_2, Hoskin et al. 2000). This is a critical observation, as it highlights the disequilibrium survival of zircon xenocrysts in rocks formed from zircon-undersaturated magmas.

Inherited zircons are also encountered in plutons of the Bega Batholith, but are here thought to represent undissolved relics of a meta-igneous source. Chen and Williams (1990) identified older zircon nuclei in four microgranular enclaves in the Glenbog Supersuite (western Bega Batholith), with a 630–430 Ma population being prevalent. The same age group dominates the inherited zircons of the Kameruka Granodiorite at the opposite side of the batholith, with another prominent age cluster between 1,260 and 930 Ma and a looser grouping between 2.7 and 2.0 Ga (Williams 1992). Similar-aged zircon inheritance apparently occurs in many other Bega Batholith plutons (Williams et al. 1988, 1992). The recurrence of the 650–500 Ma zircon population implies that the protoliths to the granites formed during this interval (Williams 1992), refractory remnants of which persist as microgranular enclaves (Chen and Williams 1990). Williams (1992) speculates that these source rocks were in turn derived by reworking a 1,250- to 900-Ma-old infra-crustal underplate. However, the uniqueness of this argument is diminished by the occurrence of the same zircon age populations in the inheritance-rich cordierite granites and detrital zircons in the Ordovician turbidites (Williams et al. 1992; Maas et al. 2001). All formerly contiguous Gondwana margin sedimentary sequences are also characterised by zircons of these ages (see Veevers 2000). The sediments were possibly shed from the metaluminous granite source rocks, their extrusive equivalents, or from a provenance that records the imprint of the same thermal episodes (Williams 1992). A vastly different interpretation holds that the inherited zircons in the Bega Batholith granites are not restitic but were contributed by Ordovician metasediment (Collins 1998).

Sample details

The 'I-type' suites chosen for this study are the Jindabyne Suite of the Kosciuszko Batholith, and the Why Worry Suite and Cobargo Suite of the western and eastern Bega Batholith, respectively (Fig. 2). Despite an arc-like chemistry, the Cobargo Suite is regarded as a hallmark 'low-temperature' association (Chappell et al. 1998). Dark-coloured, igneous-looking enclaves occur in all three suites. Zircons from samples at the either end of the geochemical spectrum shown by each suite were examined, together with a representative enclave. The bulk rock geochemistry and calculated T_{Zr} for each sample is presented in Table 1.

Jindabyne Suite

The Jindabyne Suite (Hine et al. 1978) comprises a chain of tonalitic plutons that intrude the cordierite granites of the northern Kosciuszko Batholith, and are associated with several small high-Al gabbro to diorite bodies. The suite was originally promoted as a typical example of

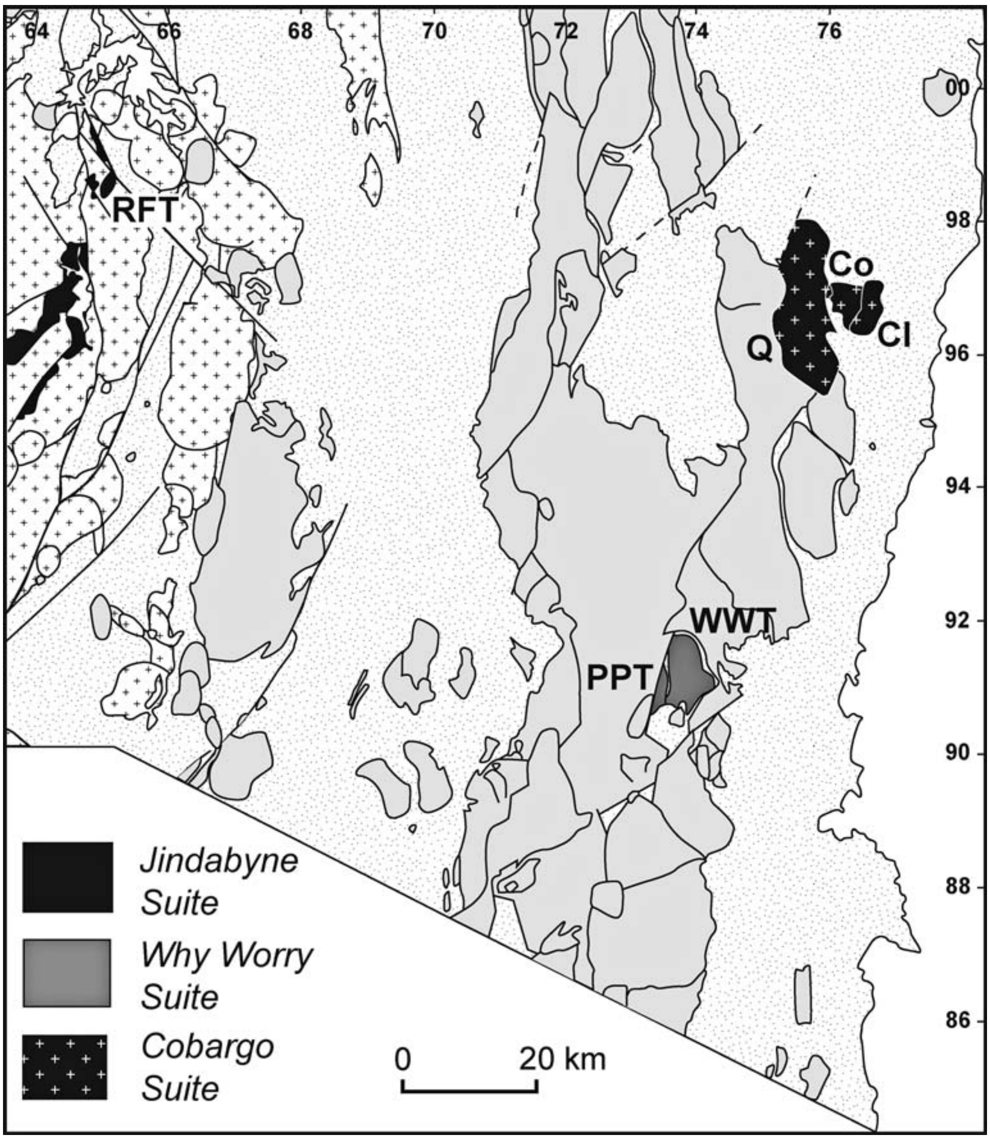

Fig. 2 Enlarged portion of Fig. 1 showing the locations of the three metaluminous suites and the plutons from which the samples were collected. Round Flat Tonalite (*RFT*); Why Worry Tonalite (*WWT*); Pretty Point Tonalite (*PPT*); Quaama Granodiorite (*Q*); Cobargo Granodiorite (*Co*); Coolagolite Granodiorite (*Cl*). Other symbols as for Fig. 1, with the *stippled pattern* denoting the country rock (mostly Ordovician and Silurian sediments)

Table 1 The major element chemistry, Zr content and calculated T_{Zr} (from Watson and Harrison 1983) for the rocks examined by this study

Rock Sample# wt%	Enclave TKB2	Enclave TKB5	Quartz diorite TKB1	Cobargo monzogranite TKB11	Enclave TKB15B	Why Worry Tonalite TKB100	Pretty Point Tonalite TKB17	Enclave RFE3	Round Flat Tonalite KK4	Round Flat Tonalite KK2
SiO_2	55.50	55.65	59.78	72.20	57.09	58.91	65.76	50.96	60.63	66.04
TiO_2	0.88	1.09	0.85	0.36	0.89	1.02	0.66	0.75	0.54	0.40
Al_2O_3	16.57	16.71	16.81	14.19	15.83	14.61	15.26	16.13	16.87	15.91
Fe_2O_3t	7.46	7.27	5.97	2.43	9.17	9.41	5.84	10.76	5.79	4.04
Fe2O3	2.18	2.33	2.13	0.86	3.17	3.18	2.11	3.58	2.11	1.69
FeO	4.75	4.45	3.46	1.41	5.40	5.60	3.35	6.46	3.31	2.12
MnO	0.13	0.15	0.09	0.03	0.13	0.15	0.08	0.23	0.11	0.08
MgO	6.60	4.98	3.45	0.95	4.00	3.70	2.07	7.10	3.37	1.90
CaO	7.66	8.03	6.35	2.44	7.71	5.60	5.43	8.21	6.28	4.45
Na_2O	3.48	4.68	3.74	3.50	2.02	1.91	2.43	1.35	2.61	3.07
K_2O	1.08	1.17	1.47	3.87	1.58	2.09	1.85	1.98	1.67	2.09
P_2O_5	0.29	0.21	0.23	0.10	0.24	0.23	0.15	0.09	0.10	0.11
ASI	0.80	0.71	0.87	0.99	0.83	0.94	0.96	0.83	0.96	1.03
M	2.43	2.74	2.03	1.49	2.19	1.80	1.63	2.42	1.76	1.51
Zr ppm	168	123	155	136	129	291	192	65	90	105
T_{Zr} (°C)	718	676	739	766	714	809	785	654	715	743

The parameter M is cationic ratio (Na + K + 2Ca)/(Al.Si). Note that T_{Zr} is only rigorously applicable to melts just saturated in zircon with $M < 1.7$. The unusually high M in the quartz diorite TKB1 compared to samples of similar silica content is attributed to the accumulation of mafic minerals. Note that samples TKB1, TKB2 and TKB5 are all from the Quaama Granodiorite

geochemical variation caused by restite unmixing, where the 'non-minimum' melt component formed at higher temperatures and by greater degrees of fusion than other restite-controlled 'minimum melt' suites (White and Chappell 1977). Samples were collected from the Round Flat Tonalite, a small (6.6 km^2) elongate body (Fig. 2) whose compositional range (60–67% SiO_2) almost spans that of the Jindabyne Suite as a whole.

The petrography of the Round Flat Tonalite is described by Hine et al. (1978) and Chappell et al. (1991), who recognise hornblende-rich and hornblende-poor variants. A sample of the former (KK4) is even-grained and dominated by complexly twinned plagioclase and hornblende prisms (to 4 mm). Plagioclase has corroded calcic cores that extend to An_{84}, which typifies all rocks of the Jindabyne Suite. Biotite tends to form single plates (2–4 mm) that enclose small plagioclase laths and may be complexly intergrown with hornblende. Aligned plates and sheaves of splintery biotite define a prominent, imposed foliation in the hornblende-poor rock (KK2), which outcrops near the southern pluton margin. Zircons in both samples are most conspicuous where they are enclosed by biotite and outlined by radiation halos.

A mafic enclave (RFE3) from the centre of the pluton comprises rectangular plagioclase (2–3 mm) and hornblende grains, many of which enclose relict augite, with minor biotite and interstitial quartz. Acicular zircons occur in both hornblende and plagioclase. The enclave is basaltic, with 50.9% SiO_2 and 7.1% MgO (Table 1). This is anomalous for metaluminous granites in general but not for the Jindabyne Suite; five other enclaves collected from the same locality are all basaltic, with between 49.5 and 52% SiO_2.

Chemically, tonalites of the Jindabyne Suite are characterised by a high-Al, low-Ti signature (Hine et al. 1978). This mirrors that of the nearby diorite and gabbro intrusions and implies a petrogenetic link between these rocks (e.g. Collins 1998). Evolved isotopic ratios are another notable feature of the Jindabyne Suite (McCulloch and Chappell 1982). For the Round Flat Tonalite, initial $^{87}Sr/^{86}Sr$ (at 415 Ma) increases from 0.7060 for the hornblende-rich KK4 to 0.7071 for the felsic sample KK2 (unpublished data).

Why Worry Suite

Encompassing the Why Worry and Pretty Point Tonalites, these rocks outcrop in the central Bega Batholith (Figs. 1, 2) and are enveloped by the screens of partially melted metasedimentary rock. The northwestern contact of the Pretty Point Tonalite is interleaved with rafts of stromatic migmatite to diatexite over several hundred metres, where the tonalite contains micaceous schlieren and variably disaggregated metasedimentary enclaves. Similar contact relationships are described for other Bega Batholith plutons (Collins et al. 2000a). The Why Worry and Pretty Point Tonalites are also intruded by swarms of syn-plutonic basaltic dykes and gabbroic bodies, and mingling and hybridisation zones occur.

The sample of Why Worry Tonalite (TKB100) is a coarse grained rock containing abundant hornblende prisms, rectangular plagioclase and masses of cloudy, bluish quartz, commonly mantled by hornblende. Distorted flakes and clots of biotite define a directional fabric, paralleled by aligned hornblende and plagioclase grains. Zircons are largely concentrated within biotite and hornblende. The Pretty Point Tonalite sample (TKB17) is texturally similar but contains less mafic minerals. A microgranular enclave (TKB15b) collected near a mingling zone within this pluton has phenocrysts of plagioclase and hornblende-ocellar quartz sparsely disseminated through a hornblende- and biotite-rich matrix. Radiating groundmass plagioclase laths are enclosed by poikilitic quartz, this being the 'pseudodoleritic' texture exhibited by microgranular enclaves in the LFB and elsewhere (Vernon 1984, 1990; Blundy and Sparks 1992; Collins et al. 2000b; Kemp 2004). Titanite and acicular apatite crystals are abundant, but zircons could not be recognised in thin section.

Despite the hornblende-rich character, the Why Worry Tonalite has among the most evolved isotopic ratios exhibited by metaluminous granites in eastern Australia, with ϵNd-6.6 and initial $^{87}Sr/^{86}Sr = 0.7080$.

Cobargo Suite

Flanking the eastern edge of the Bega Batholith, this suite comprises the Coolagolite, Cobargo and Quaama Granodiorites, all of which intrude hornfelsed Ordovician turbidites. The Quaama Granodiorite also crosscuts the 421 Ma Kameruka Granodiorite to the west (Williams 1992). Relative to other Bega Batholith suites, the Cobargo Suite plutons are distinguished by a quartz-poor character and are compositionally zoned (Lewis et al. 1994). The Cobargo Granodiorite varies from an outer zone of quartz monzodiorite to felsic microgranite, whereas the Quaama Granodiorite grades from quartz diorite at its eastern periphery into felsic granodiorite and monzogranite towards the pluton centre. Zoned plutons are uncommon in the LFB and typically form by fractional crystallisation (e.g. Bateman and Chappell 1979), as inferred for the Boggy Plain intrusive (Wyborn et al. 2001). The quartz diorite at the margin of the Quaama Granodiorite contains swarms of enclaves, including pyroxene- and hornblende-rich bodies (up to 1 m) and angular hornfels xenoliths. Cobargo Suite rocks are also intruded by intermediate to felsic dykes, some of which have high Zr contents (up to 330 ppm). These plausibly belong to the Cobargo Suite, although some could be related to felsic 'A-type' magmatism further east.

The quartz diorite (TKB1) is dominated by blocky, closely packed plagioclase laths (to 7 mm, An_{50}–An_{30}), between which are masses of brown-green hornblende, large biotite plates and interstitial quartz and rare orthoclase. This texture suggests that the rock is plagioclase-accumulative. Many hornblende grains enclose augite, and orthopyroxene relicts occur within rectangular cummingtonite sheaves, which are fringed by actinolite and perforated by blebs of magnetite and ilmenite. Zircons occur close to grain boundaries (Fig. 3a), implying late crystallisation.

The felsic Cobargo Suite rock (TKB11, Cobargo Granodiorite) is a porphyritic monzogranite, where hornblende and plagioclase phenocrysts (to 1 cm) are sparsely distributed through a felsic, microgranitic matrix. Poikilitic orthoclase is conspicuous in thin section.

Two enclaves were collected from the quartz diorite, and although both have ~55% SiO_2, they are lithologically contrasting. Sample TKB2 is a medium- to coarse-grained diorite, where aggregates of blocky plagioclase grains (~5 mm), orthopyroxene prisms and amphibole-rimmed augite masses occur in a finer groundmass of plagioclase and pyroxene laths, interstitial to poikilitic hornblende, biotite and minor quartz. Chlorite ovoids in the centre of orthopyroxene are possibly after olivine. The larger plagioclase grains occasionally contain irregularly shaped cores (to $\sim An_{60}$) that are outlined by tiny trains of pyroxene crystals. This feature also occurs in the granitic rocks (Chappell et al. 1991), though the plagioclase becomes less calcic (e.g. cores of An_{40}–An_{450} in the quartz diorite TKB1). Zircons in the diorite are localised along plagioclase grain boundaries (Fig. 3b) or embedded within interstitial amphibole. Enclave TKB5 is more typical of microgranular enclaves within the LFB granites. It has plagioclase phenocrysts and rectangular clinopyroxene grains (1–1.5 mm, mantled by hornblende) dispersed through a matrix of spindly biotite and hornblende, plagioclase laths and interstitial quartz. Zircons are irregularly shaped and interstitial (Fig. 3c).

The Cobargo Suite is distinguished by relatively high Na_2O and Sr contents, which typifies subduction-related tonalites of magmatic arcs (Chappell and Stephens 1988). Accordingly, the isotopic compositions of Cobargo Suite plutons are more primitive than those of the Why Worry or Jindabyne Suites. The quartz diorite sample has ϵNd + 0.6 and initial $^{87}Sr/^{86}Sr = 0.7047$, identical to the values quoted for the Coolagolite Granodiorite by Chappell et al. (1991). There is no published ion microprobe data for zircons of the Cobargo Suite, although Chappell et al. (1991) state that of 64 zircons inspected from the Coolagolite Granodiorite, two contain inherited cores.

Analytical techniques

Zircons were separated from 1 to 5 kg of pulverised rock by conventional heavy liquid and magnetic separation techniques. Approximately 200–250 grains from each sample were mounted in epoxy resin and ground and polished to expose their interior. Zircons of assorted morphologies were selected, and all were carefully characterised by cathodoluminescence (CL) and back-scattered electron imaging before ion microprobe analysis.

The U-Pb data (Electronic Supplementary Table 1) were obtained with a Cameca ims1270 ion microprobe housed at the Swedish Museum of Natural History, Stockholm. The operating conditions and analytical protocols are essentially the same as those outlined by Whitehouse et al. (1997), but including the modifications described by Whitehouse et al. (1999). The Pb/U calibration was performed relative to the 1065-Myr-old

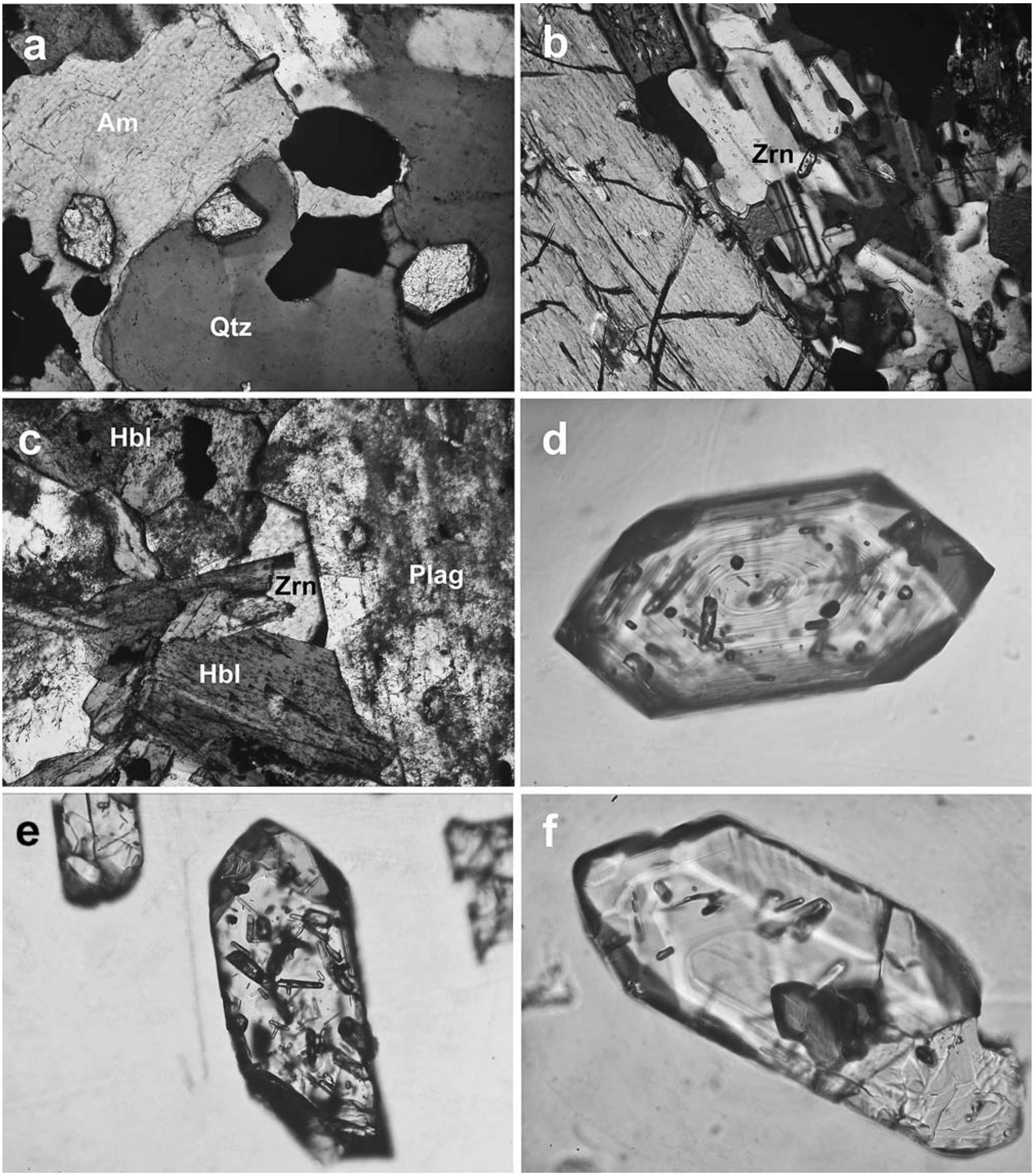

Fig. 3 Photographs of zircons from the Cobargo Suite. **a** Three zircons (high relief) in the quartz diorite TKB1, occurring inside interstitial quartz (*Qtz*) or amphibole (*Am*). Crossed polars, long edge of photo 1.8 mm. **b** Small zircon crystal (*Zrn*) located within the finer matrix of diorite enclave TKB2 adjacent to an orthopyroxene phenocryst (*left*). Crossed polars, long edge of photo 1.0 mm. **c** Anhedral interstitial zircon in microgranular enclave TKB5. Plane light, long edge of photo 1.0 mm (Hbl, hornblende; Plag, plagioclase). **d** Zircon (250 μm longest dimension) in Cobargo monzogranite showing strong oscillatory zoning and numerous apatite inclusions. **e** Zircon crystal in the diorite TKB2 (320 μm long) hosting inclusions of pyroxene (high relief elongate grains), apatite needles and a rectangular plagioclase grain (*top right* of zircon). **f** Biotite plate within an irregularly shaped zircon (200 μm long) from the diorite enclave TKB2

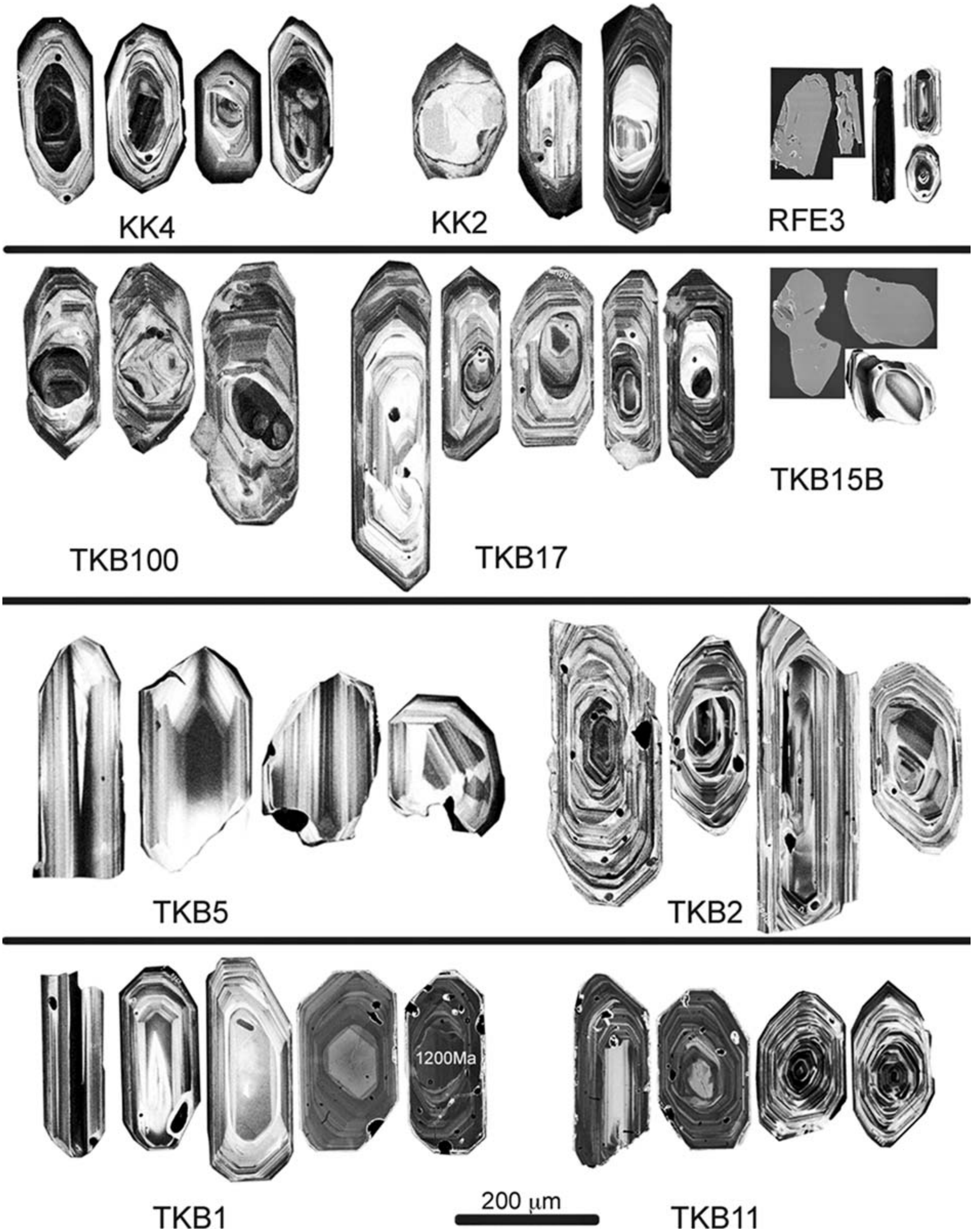

Fig. 4 Cathodoluminescence images of selected zircon crystals from each sample. BSE images (*greytones*) are also included for the Cobargo quartz diorite (*TKB1*) and monzogranite (*TKB11*), and secondary electron images for enclaves RFE3 and TKB15. All grains are shown at approximately the same scale. Note the conspicuous inherited cores of the Why Worry Tonalite (*TKB100*), and the larger inherited cores of the felsic Round Flat Tonalite (*KK2*) compared to the hornblende-rich sample KK4

Geostandards zircon 91500 (Weidenbeck et al. 1995), which was analysed repeatedly throughout each session. As a secondary check on this calibration, analyses of the Temora 2 standard zircon were also interspersed during one session and yielded a weighted average $^{206}Pb/^{238}U$ age of 416.4 ± 4.5 Ma (95% confidence, $n = 14$, MSWD = 0.65) indistinguishable to that quoted by Black

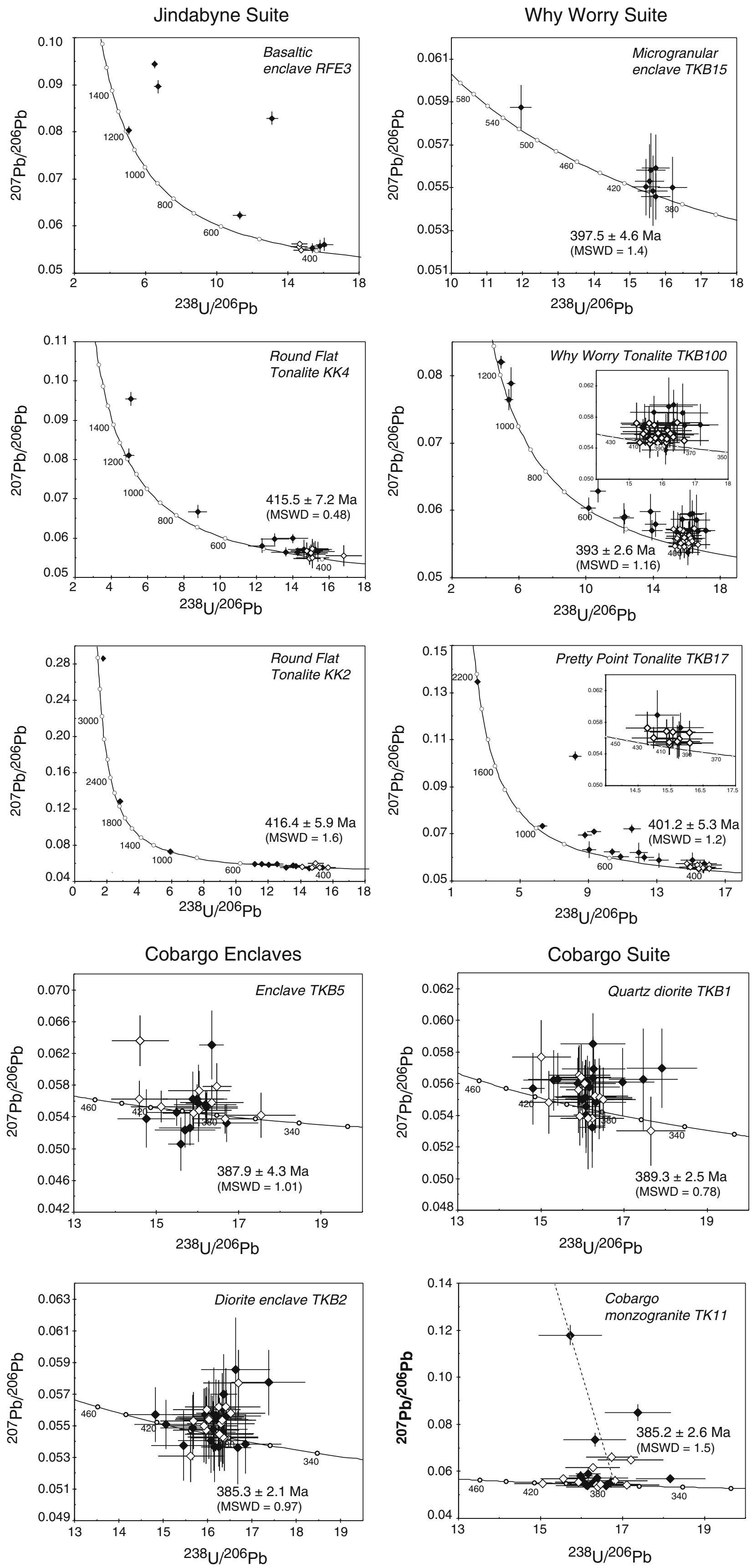

Fig. 5 Tera-Wasserburg concordia diagram of zircon U-Pb isotopic compositions from the Jindabyne, Why Worry and Cobargo suites. Data are uncorrected for common Pb and are plotted with 2σ *error bars*. *Filled circles* are from zircon cores, *open symbols* from rims. The inferred magmatic crystallisation age for each sample (average $^{206}Pb/^{238}U$ age corrected for common lead) is also indicated, and the projection to common lead of Stacey and Kramers (1975) is shown for the most discordant zircon of sample TKB11. Analyses of one inherited core from TKB1 (Pb/U age ~1250 Ma) and a zircon rim showing severe lead loss from KK2 (~283 Ma) are not shown

et al. (2004). All magmatic ages are quoted at 95% confidence limits (i.e. $t\sigma$ where t is 'Student's t test') and represent weighted averages of $^{206}Pb/^{238}U$ ages corrected for common lead contamination by the ^{207}Pb method (computed by 'Isoplot', Ludwig 2001), whereby each analysis is extrapolated to concordia along a mixing line projected from the present-day terrestrial lead composition of Stacey and Kramers (1975) ($^{207}Pb/^{206}Pb = 0.83$, with an arbitrary error of ± 0.1). These corrections are typically small relative to the analytical error on each measurement. Analyses that clearly show the effects of age inheritance or radiogenic lead loss, as manifest by anomalously old or young $^{206}Pb/^{238}U$ ages, respectively, or those few analyses with elevated common lead, were excluded from magmatic age calculations. Outlier rejection was otherwise made where subsequent examination revealed that the ion beam traversed cracks or overlapped texturally disparate regions within the grain (e.g. mixed core-rim analyses). The analytical strategy was directed towards identifying inherited components, so that zircon cores were preferentially targeted.

Results

Jindabyne Suite

Zircons from the Round Flat Tonalite sample KK4 are pale pink, squat to equant crystals showing subequal development of both (100) and (110) prisms and (101) and (211) pyramidal terminations (Fig. 4). Inclusions are uncommon, but rounded cores with a cloudy aspect are discernible in some grains under optical microscopy. Analyses from the oscillatory-zoned zircon rims yield a weighted average of 415.5 ± 7.2 Ma (MSWD = 0.48, Fig. 5), which dates magmatic crystallisation. Obvious Pb-loss is seen in a single rim analysis (Pb/U age ~373 Ma). Six zircons contain large euhedral to moderately embayed cores that exhibit a light mottled appearance in CL and have $^{206}Pb/^{238}U$ ages that are indistinguishable from those of the zircon rims. These plausibly represent an early generation of magmatic zircon growth. However, most cores are smaller, generally darker in CL than their overgrowths and show greater rounding and truncation of internal zonation. These cores have pre-magmatic ages that are clustered at ~450–480 Ma, with single cores at 500, 700, and 1,200 Ma (Fig. 5). One strongly discordant core is probably at least as old as its $^{207}Pb/^{206}Pb$ age of ~1,540 Ma.

Zircons from the felsic Round Flat Tonalite (KK2) exhibit greater cracking and have lower optical clarity, possibly manifesting deformation. They differ from those of the hornblende-rich sample KK4 in having higher aspect ratios and showing greater development of the (110) prism (Fig. 4). A cluster of analyses deriving from the rims of these zircons yield an inferred crystallisation age (416.4 ± 5.9 Ma, MSWD = 1.7). This is equivalent to that of sample KK4, and combining all rim data for both rocks gives the best age estimate for the Round Flat Tonalite at 416.1 ± 4 Ma (MSWD = 0.87). Some zircons in KK2 also contain rounded cores that are distinctly larger than those of KK4. These are predominantly inherited, defining age groups at 450 and 500–550 Ma (four cores each), with single, near-concordant cores of approximately 1,000 and 2,000 Ma and a discordant core with a $^{207}Pb/^{206}Pb$ age of 3,400 Ma (Fig. 5). In general terms, these age distributions (and those of the Why Worry Tonalite, see below) typify inherited and detrital zircons in the LFB (Fig. 6). Given the internal fractures, at least some of the scatter along concordia shown by the youngest inherited population might be due to minor lead loss.

The rare zircons within the enclave RFE3 display two distinct morphologies (Fig. 4). The dominant type is of elongate to acicular brown crystals (some > 400 μm in length), many of which exhibit irregular, skeletal outlines. They contain large euhedral cores that are uniformly dark in CL, or show a vague mottling. The cores are thinly mantled by a CL bright zone, in turn rimmed by a dark euhedral shell. Although only three of these zircons were amenable to analysis, the Pb/U ages overlap the magmatic age of the host tonalite (Electronic Supplementary Table 1, Fig. 5). They are further distinguished by high U and Th contents and elevated Th/U ratios (> 1.6) compared to the host tonalite, where the magmatic zircon has Th/U ratios below unity (Electronic Supplementary Table 1). This could reflect the lack of co-precipitation with U- and Th-rich accessory phases, such as allanite. The second type of zircons resemble those of

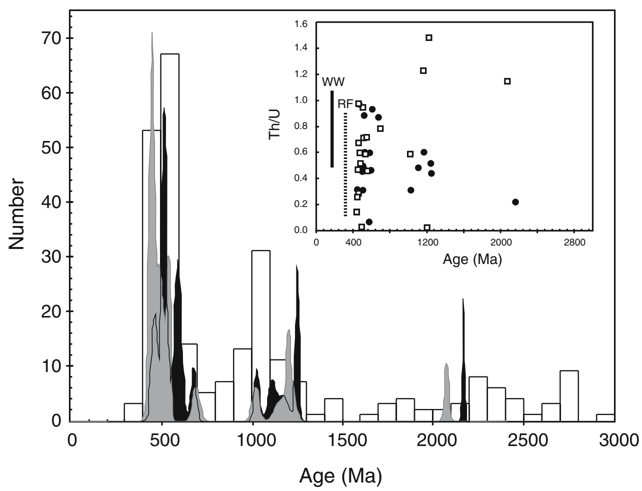

Fig. 6 Cumulative gaussian probability curves comparing inherited zircon age spectra from the Jindabyne (*grey shade*) and Why Worry (*filled*) Suites with the age distributions of detrital zircons from the low-grade LFB Ordovician metasediments (*histogram*; pooled dataset of Keay et al. 1999 and Williams 2001). The $^{207}Pb/^{206}Pb$ age is used for granite-hosted zircons exceeding 1.5 Ga; all others represent $^{206}Pb/^{238}U$ ages corrected for common lead by the ^{207}Pb method. Strongly discordant grains (i.e. well outside analytical error) are omitted. The *inset* shows the Th/U ratios of inherited grains compared to the range showing magmatic zircons from the same rock (Round Flat Tonalite, *open squares*; Why Worry Tonalite, *filled circles*). Inherited grains in the Why Worry Suite extend to lower Th/U ratios than magmatic zircons, though there is no systematic relationship between Th/U ratio and age

the tonalite but are much smaller (< 100 μm). With one exception, analysis of the centre of these grains yields grossly discordant pre-magmatic ages, reflecting mixed contributions from older cores and magmatic rims. The rims themselves give slightly younger ages than the crystallisation age of the host tonalite (Table 1).

Why Worry Suite

These tonalites contain stubby-to-elongate pinkish zircons that are dominated by the (100) prism (Fig. 4). Inclusions are common, and, in order of abundance, they range from apatite, titanite, magnetite and plagioclase. Thirty-five zircons were analysed from the Why Worry Tonalite (TKB100), from two separate probe mounts containing large (> 200 um) and small (< 200 um) size fractions. Concordant analyses from rims of the smaller zircons yield a tightly constrained magmatic age of 394 ± 3.8 Ma (n = 10). In contrast, the larger zircons show evidence for isotopic disturbance of both magmatic grains and a young (< 600 Ma) inherited component. Nine analyses from rims overlap the age of the smaller zircon fraction, whereas one younger rim analysis reflects Pb loss following crystallisation. Two discordant rim analyses were rejected. Nine euhedral to subhedral cores were analysed, which (besides two discordant analyses) plot within error of the magmatic age. These cores probably manifest an early phase of melt-precipitated zircon, although the possibility that some are isotopically disturbed inherited nuclei cannot be precluded. Pooling overlapping analyses from both size fractions defines a crystallisation age for the pluton of 393.0 ± 2.6 Ma (n = 26, MSWD = 1.16).

Inherited cores have a rounded morphology and exhibit a CL and zoning contrast with their magmatic overgrowths, many being unzoned or having an irregular, patchy zonation (Fig. 4). Many are recognised optically by a greater density of apatite needles. Ten of these cores have slightly discordant ages between 440–500 Ma (four analyses), ~600 Ma (two analyses) and 1,070–1,190 Ma (four analyses) (Fig. 5). Five anhedral cores yield discordant ages that either overlap or are younger than the inferred magmatic age of the tonalite. These are interpreted as pre-magmatic components that have lost radiogenic lead.

Zircons within the Pretty Point Tonalite also have prominent age inheritance (Fig. 5). Most analyses are concentrated around 400 Ma (including three euhedral cores), defining a magmatic age of 401.2 ± 5.3 Ma (n = 13, MSWD = 1.2). There is little evidence for U-Pb isotopic disturbance within this population. As with the Round Flat and Why Worry tonalites, inherited cores are dominated by the 500–600 Ma age group, with two grains at 680–690 Ma and cores at ~950 and 2,150 Ma. Two analyses are significantly displaced from concordia and thus their true age cannot be reliably ascertained.

Only eight small (< 100 μm) zircons could be analysed within the microgranular enclave TKB15b. All of these show varying degrees of embayment, rounding and/or corroded surfaces (Fig. 4), which suggest that they were being resorbed by the host magma. The enclave magma therefore must have been zircon-undersaturated, consistent with its low Zr content (130 ppm). Concordant analyses from seven grains yield an age of 397.5 ± 4.6 Ma (MSWD = 1.4), which agrees with that of the host tonalite. The eighth grain returns an age of ~520 Ma, and thus is a fragment of an inherited component, though unusually this grain lacks evidence of a younger, melt-precipitated rim. These data suggest that the zircons in the enclave TKB15b are xenocrysts and that they were probably entrained from the juxtaposed tonalite magma during mingling.

Cobargo Suite

The quartz diorite TKB1 contains short prismatic zircons that are dominated by a single (100) prism face, with (110) either absent or weakly developed (Figs. 3a, 4). The (101) pyramid is mostly more prominent than (211). In general, this crystal form typifies zircons from high-temperature alkaline to tholeiitic igneous rocks (Pupin 1980; Corfu et al. 2003). Many zircons contain euhedral to sub-rounded cores that lack internal zoning. Perceptible cores are absent from other grains, which instead exhibit broad oscillatory zoning around tiny inclusions (apatite or magnetite) located at their centres. Elongate zircons are sector zoned.

Irrespective of morphology or location within the zircon, most ion probe analyses are concordant and cluster around 390 Ma, from which a weighted average age of 389.3 ± 2.5 Ma (n = 27, MSWD = 0.78) constrains the crystallisation age of the quartz diorite (Fig. 5). Slight lead loss is suspected for three grains (two being cores) with clearly lower $^{206}Pb/^{238}U$ ratios, whereas two analyses whose age (415–420 Ma) marginally exceeds the inferred magmatic age are treated as analytical outliers. A single core, distinguished by an irregular outline (Fig. 4), yields a pre-magmatic age of ~1,250 Ma.

The Cobargo monzogranite TKB11 has yellowish zircons that exhibit slightly greater development of the (211) crystal form. Many grains are crowded with apatite needles and exhibit strikingly fine oscillatory zoning around tiny euhedral to rounded cores (Figs. 3d, 4). Age calculations, including analyses from zircon centres, distinguish a single age population of 385.2 ± 2.6 Ma (n = 22, MSWD = 1.5). Six grains (three cores, three rims) have elevated $^{207}Pb/^{206}Pb$ ratios relative to concordia and define a chord towards the composition of common Pb (Fig. 5). SEM inspection of the zircons reveals that the ion probe pits of the three cores impinged upon cracks radiating from mineral and crystallised melt inclusions, from where the common Pb contaminant may have been incorporated.

The two enclaves sampled from the Quaama Granodiorite contain wholly melt-precipitated zircon populations. Enclave TKB5 has large (to 500 μm) blocky to elongate brownish zircons (Fig. 4), most of which were broken during separation. They exhibit simple, broad oscillatory to sector zoning, sometimes with euhedral cores, reflecting single-phase growth. Both euhedral and repressed crystal faces are developed. These features characterise zircons formed by late-stage crystallisation from evolved interstitial melt pools in magmas that were initially undersaturated in Zr (e.g. Hoskin 2000; Corfu et al. 2003). The elongate grains contain microcrystalline tubes, possibly devitrified melt inclusions, parallel to the *c*-axis. Ion probe analyses of the zircons have a weighted average of 387.9 ± 4.3 Ma (n = 18, MSWD = 1.01), rejecting four outliers (Fig. 5).

Zircons within the diorite enclave TKB2 are dominated by the (100) prism and are densely packed with inclusions, mostly apatite (Fig. 3e, f). These are concentrically arranged with respect to the pronounced oscillatory zoning. Inclusions of plagioclase, pyroxene, magnetite and biotite, accompanied by devitrified melt blebs, testify to late crystallisation. Most grains either lack cores or have unzoned euhedral centres. However, several zircons contain conspicuous rounded cores whose oscillatory zoning is truncated by that of the rims and thus represent an earlier zircon growth stage. Regardless of internal morphology, U-Pb ages are tightly clustered (Fig. 5) and yield a weighted average of 385.3 ± 2.1 Ma (n = 38, MSWD = 0.97). Like the enclave TKB5, zircons in TKB2 crystallised synchronously with the enclosing quartz diorite magma. These enclaves are therefore fragments of a coeval magma or igneous rock, rather than older, meta-igneous restite.

Implications for LFB granite genesis

The three metaluminous tonalite suites show clear differences in both the morphologies and U-Pb age populations of their constituent zircons. Moreover, these suites produce quite different trends on plots of bulk rock Zr concentration and calculated T_{Zr} versus silica, although they converge in the most evolved compositions (Fig. 7). Most striking are the steep negative trends for both Zr content and T_{Zr} defined by rocks of the Why Worry Suite, which have the greatest proportion of zircon inheritance. In contrast, Zr and T_{Zr} show the opposite pattern and increase with silica in the Jindabyne Suite, which has less inheritance. Rocks of the virtually inheritance-free Cobargo Suite fall between these extremes, showing an increase in T_{Zr}, but moderate decrease in Zr content with evolution to higher silica. In all three cases the T_{Zr} of the lower silica rocks are below the temperatures of such magmas at the onset of crystallisation, whereas the T_{Zr} in the most felsic samples are broadly similar and appropriate for liquids of these compositions. The following discussion will explore the extent to which the inter-related patterns of Zr, T_{Zr} and zircon inheritance can be deconvolved for the three granitic suites to gain insight into magmatic temperatures and the processes involved in magma generation. The two suites with the pre-magmatic zircons are considered first.

Case 1: the Why Worry Suite

These tonalites appear to present a straightforward scenario. The conspicuous zircon inheritance, combined with the steep decrease in Zr content and T_{Zr} with evolution to higher silica, is compatible with zircon separation. Such zircon presumably included both inherited and melt-precipitated crystals. However, the calculated T_{Zr} is too low to reflect the onset of liquidus

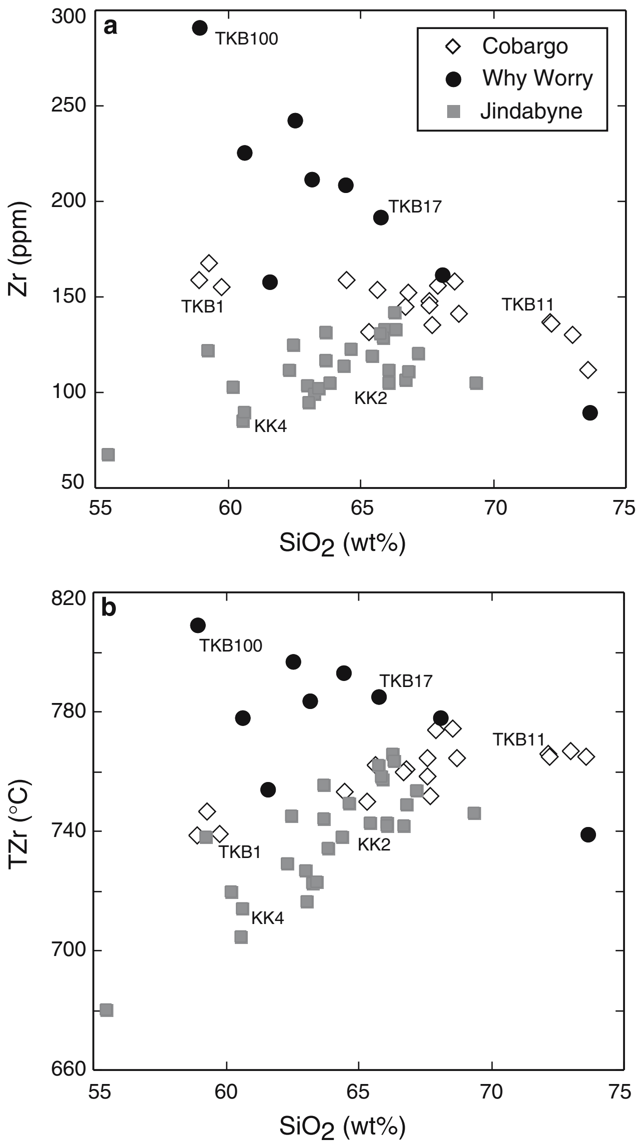

Fig. 7 **a** Zr-SiO_2 variation diagrams for the hornblende-bearing Jindabyne, Why Worry and Cobargo Suites of the LFB. Data are from Hine et al. (1978), Chappell et al. (1991) and this study. **b** Plot of T_{Zr} (from Table 1) versus SiO_2 for the three suites. The samples whose zircons were analysed by this study are labelled

crystallisation, and so we infer that zircon saturation occurred within a magma that was already partially solidified. The nature of the suspended crystals bears significantly on models for granite formation. They could be restite from the inferred meta-igneous protolith, or melt-precipitated phases that reflect the differentiation of the host magma. Each has different implications for initial magmatic temperatures, but in both cases, T_{Zr} is an unreliable measure of the temperature at which zircon saturation occurred (but see Miller et al. 2003).

As previously emphasised (e.g. Vernon 1983; Wall et al. 1987; Collins 1998), the petrographic evidence for the recognition of restitic minerals in metaluminous granites is equivocal. This is equally true of enclaves, and we note that the textures and zircon morphologies of enclave TKB15b accord with a magma mingling, instead of restitic, origin (cf. Chen and Williams 1990). Pre-magmatic zircons are the best candidates for restite, and imply that magma generation proceeded in the zircon stability field (Chappell et al. 1998, 2000). In this case, the pattern of Zr variation in the Why Worry Suite should be controlled by restitic zircon, but a simple calculation shows that this is untenable. The Why Worry Tonalite TKB100 is the most mafic rock of the suite, and in the restite scenario it therefore contains just enough melt to form a mobile magma (~40% melt, 60% restite). The abundance of zircon in this rock is estimated at ~0.05%, using the method of Sawka and Chappell (1988); this calculation assumes 0.1 vol% zircon for every 700 ppm Zr in the whole rock and tends to overestimate actual zircon abundance (Sawka 1988). Inherited cores occur in ~60% of zircons in TKB100 (gauged from both ion probe analysis and visual inspection of CL images) and comprise, at most, one-third of the grain (see Fig. 4). This translates to merely 65 ppm Zr in the restite assemblage, which is clearly insufficient to produce the negative trend on Fig. 7, unless zircon was also crystallising from the melt. The latter is unavoidable if the melt was generated in equilibrium with residual zircon, but then this becomes fractional crystallisation, rather than restite unmixing. Another test is that since rock compositions are interpreted as restite-melt mixtures, they should define straight lines on element-element plots. For the Why Worry Suite, this does not always appear to be true (Fig. 8). For these reasons, we conclude that a simple restite unmixing model is not applicable here.

The preferred interpretation is that the crystals in the Why Worry Suite precipitated from molten magma at higher temperatures than T_{Zr}. In this case, the inherited zircons are not restitic but were entrained from the surrounding migmatitic metasediments at a stage in the solidification history when zircon was insoluble and crystallising at sub-liquidus temperatures. This accords with the field relationships and the evolved isotope ratios of the Why Worry Suite. The steep linear decrease in Zr content, and thus T_{Zr}, reflects the separation of zircon that formed relatively late in the crystallisation sequence, together with variable amounts of other minerals present in the magmas at that stage.

Case 2: the Jindabyne Suite

The apparent paradox of the Jindabyne Suite is that while the presence of inherited zircons implies that the magmas were zircon-saturated, the broad increase in Zr concentration and T_{Zr} with silica typifies high-temperature suites where zircon is soluble (e.g. Chappell et al. 2000). As noted earlier, the Jindabyne Suite is particularly significant in the context of granite genesis in defining a typical example of restite unmixing. In such a model, the Zr content of the felsic melt component must have exceeded that of the restite, consistent with the minor zircon inheritance detected in the Round Flat Tonalite. The paucity of inherited zircon could in turn reflect higher temperatures of formation (Chappell et al. 1987) and thus greater dissolution of zircon in the source, which can be assessed further.

The end-member melt component in the restite model is approximated by the most felsic rocks of the suite that are unmodified by crystal fractionation, and for these, T_{Zr} is a reasonable proxy for magma temperature. According to the restite model, this temperature should also apply for lower silica samples of the suite, which have acquired that character only by greater retention of mafic restite. The putative felsic melt composition may be best represented by sample KB7 of Hine et al. (1978), which has 67.2% SiO_2 and a T_{Zr} of 755°C. Yet, this temperature resembles that of leucogranites produced by muscovite-melting reactions (e.g. Patiño Douce and Harris 1998), and is almost certainly too low for a 'non-minimum melt' hornblende tonalite with 60% SiO_2. Indeed, much higher temperatures are required for the

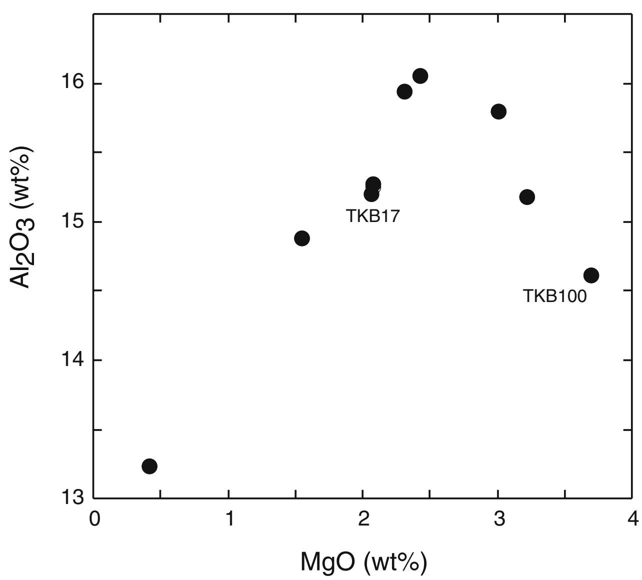

Fig. 8 Plot of Al_2O_3 versus MgO for rocks of the Why Worry Suite

melt to be in equilibrium with the anorthitic plagioclase of the Jindabyne Suite. According to the model of Burnham (1992), the temperature at which An_{80} plagioclase and quartz co-exist as liquidus phases for the Jindabyne Suite is ~950°C, although this drops with increasing melt-water content. The elevated P_2O_5 contents (>0.1%) of the felsic Jindabyne rocks also suggest higher temperatures, since at 755°C KB7 can only dissolve ~0.03% P_2O_5, even allowing for the enhanced apatite solubility in mildly peraluminous melts (Bea et al. 1992). The apatite saturation temperature of this rock is nearly 870°C, according to the formulation of Bea et al. (1992). Although they are approximations, these calculations highlight the difficulties with the inferred low temperatures of the Jindabyne Suite magmas if they are zircon saturated.

An alternative is that the Jindabyne magmas were initially undersaturated in zircon and that some differentiation took place before zircon crystallised. Two scenarios are possible. Wall et al. (1987) argue that chemical variation within the Jindabyne Suite could be accomplished by fractional crystallisation from a dioritic to tonalitic parent, where the tonalites approximate derivative liquids and the associated gabbros are the complementary cumulates. The positive Zr-SiO_2 trend denotes that zircon was not an early liquidus phase, consistent with the low T_{Zr} of the mafic Round Flat Tonalite, and that this increases with SiO_2. However, the presence of similarly calcic plagioclase cores throughout the Jindabyne Suite suggests that minerals were separated from the liquid in different proportions to those in which they crystallised, and/or the back-mixing of differentiated melts with early cumulates occurred (Wall et al. 1987).

The second possibility is that the Jindabyne Suite trends reflect the progressive partial melting of a mafic to intermediate precursor analogous to the high-Al gabbros. The calcic plagioclase cores might be restitic from the source rocks (e.g. Chappell et al. 1987), but the melts were not in equilibrium with zircon, which either was absent from the protolith or eliminated early during melting. In any case, the lower Zr content of the most silicic Jindabyne sample (69.5% SiO_2, $T_{Zr}=746$°C) probably signals the onset of zircon fractionation.

A corollary of both crystallisation and partial melting models is that the inherited zircons in the Jindabyne Suite are xenocrysts derived by assimilation of older crust, and were metastably preserved in a hotter magma than registered by the T_{Zr}. This accords with the increase in initial $^{87}Sr/^{86}Sr$ from 0.7061 to 0.707 with silica in the Round Flat Tonalite, which can be achieved by 12% bulk assimilation of average Ordovician metasediment, or 20% assimilation of the surrounding cordierite granite (using the data of McCulloch and Chappell 1982). The inherited zircons are undigested relics of the contaminant, consistent with their preponderance and greater size in the felsic tonalite sample. Rounding and embayment of the cores manifests resorption, which was arrested either by cooling of the magma or by the attainment of zircon saturation in the localised environment of the crystal (e.g. within a shrinking melt pool).

The behaviour of zircon during magmatic events has been modelled by Watson (1996). Zircon dissolution is shown to depend on an interplay among the thermal history, the degree of melt undersaturation in zircon, the volume of the interacting melt reservoir, and the size of the grain and its time in contact with Zr-poor melt (Watson 1996). Simulations reveal that only large zircons (>120 μm) would survive intense (>850°C) anatectic events on geologically reasonable time-scales. However, it is harder to predict how zircon xenocrysts might respond during the assimilation of crust by a crystallising, Zr-undersaturated magma. Zircons in metasedimentary rocks are commonly encapsulated by micas (Bea 1996) and so could be occluded from the melt until late in the crystallisation sequence. Upon their release into a partially solidified pluton, these xenocrysts would form substrates for magmatic zircon growth from the felsic residual liquid. The oscillatory-zoned rims around inherited cores do not necessarily denote a protracted magmatic residence time, but form rapidly in response to localised zircon-supersaturation in a highly polymerised silicic liquid (Vavra 1990; Hoskin 2000). The Boggy Plain intrusion demonstrates the survival of zircon xenocrysts in an originally zircon-undersaturated melt, where these have acquired melt-precipitated overgrowths. Together with the Jindabyne example, this underlines the pitfalls in inferring source temperatures based on zircon age inheritance alone.

Origin of enclaves in the Round Flat Tonalite

The basaltic compositions and textures suggest that these are intermingled fragments of hybridised mafic magma, and, as with the enclave in the Pretty Point Tonalite, this conforms to the zircon populations in enclave RFE3. The elongate, skeletal zircon morphology reflects nucleation and growth during undercooling (Corfu et al. 2003), as induced by the quenching of a hot mafic magma globule within a cooler, felsic host (Elburg 1996). Rapid crystallisation would result in a framework of high-temperature minerals immersed in interstitial Zr-rich liquid. The acicular zircons probably crystallised from pockets of the latter, perhaps where localised saturation was attained at the interface of a growing Zr-poor mineral, like plagioclase (Bacon 1986). The high Th/U ratios of these grains typify zircons that have crystallised from mafic melts (e.g. Amelin 1998). The smaller, equant zircons with older cores are interpreted as xenocrysts entrained from the tonalite during intermingling. Their minimal resorption indicates either that the enclave melt was approaching zircon saturation at the time the grains were incorporated, or that zircon dissolution was outpaced by crystallisation of the enclave.

Case 3: the Cobargo Suite

This suite exemplifies the intriguing and petrogenetically informative situation where Zr content falls with increasing silica, implying zircon crystallisation, but T_{Zr} actually rises (Fig. 7). Chappell et al. (1991) report the presence of inherited zircons in this suite; yet, of nearly 1,000 zircons inspected from four Cobargo Suite rocks, only one inherited core was detected, despite a conscious search for such a component. The case for the Cobargo magmas having been zircon-saturated at the source is therefore tenuous. The petrographic evidence for late zircon crystallisation noted above also militates against early zircon saturation.

A key feature of the Cobargo Suite is the curved arrays defined by incompatible elements, like Rb and Th (Fig. 9), which are strengthened if several spatially associated gabbro and diorite bodies and mafic enclaves are included. These trends cannot be reconciled by simple mixing or unmixing processes but are instead diagnostic of granitic suites whose evolution is governed by fractional crystallisation. Similarly, if data from the mafic and granitic rocks of the Cobargo Suite are combined, the resulting pattern of Zr variation shows an inflection near 61% SiO_2 (Fig. 9c) that is consistent with the onset of zircon precipitation from an evolving magma. This pattern closely resembles that shown by 'high-temperature' suites like Boggy Plain. The point of zircon saturation in the Cobargo Suite is poorly defined due to a compositional gap between 60 and 65% SiO_2, but the felsic rocks that define the negative part of the trend occupy the same silica range as the Boggy Plain monzogranites that were formed from zircon-saturated melts. The morphological trend of zircons in the Cobargo Suite, such that zoning becomes more intricate as the rocks become more felsic, is precisely as exhibited by the zircons of fractionated intrusives, and is linked to precipitation from increasingly polymerised melts as differentiation proceeds (Hoskin 2000).

Nevertheless, it is unlikely that the Cobargo Suite formed as a series of fractionated liquids. This is because of the fact the T_{Zr} for the lower silica, supposedly zircon-saturated rocks of the suite (~740°C), is far too low for melts of these compositions (Chappell et al. 1998). The increase in T_{Zr} with silica is also not expected for zircon-saturated magmas (e.g. Sawka 1988; Hoskin et al. 2000). Moreover, the moderate decrease in Zr following the inflection argues against the efficient removal of melt-precipitated zircon; this would deplete the melt much more rapidly in Zr, as shown by fractionation-controlled suites (Fig. 9c). In part, this reflects the plummeting solubility of zircon with falling temperature and in increasingly silicic melts (Watson and Harrison 1983).

Instead, we consider that the zoned Cobargo plutons solidified from mixtures of variably differentiated melt and precipitated liquidus phases during in situ crystallisation, in analogous fashion to that proposed for the Boggy Plain pluton (Wyborn et al. 2001). A model for this is elaborated below.

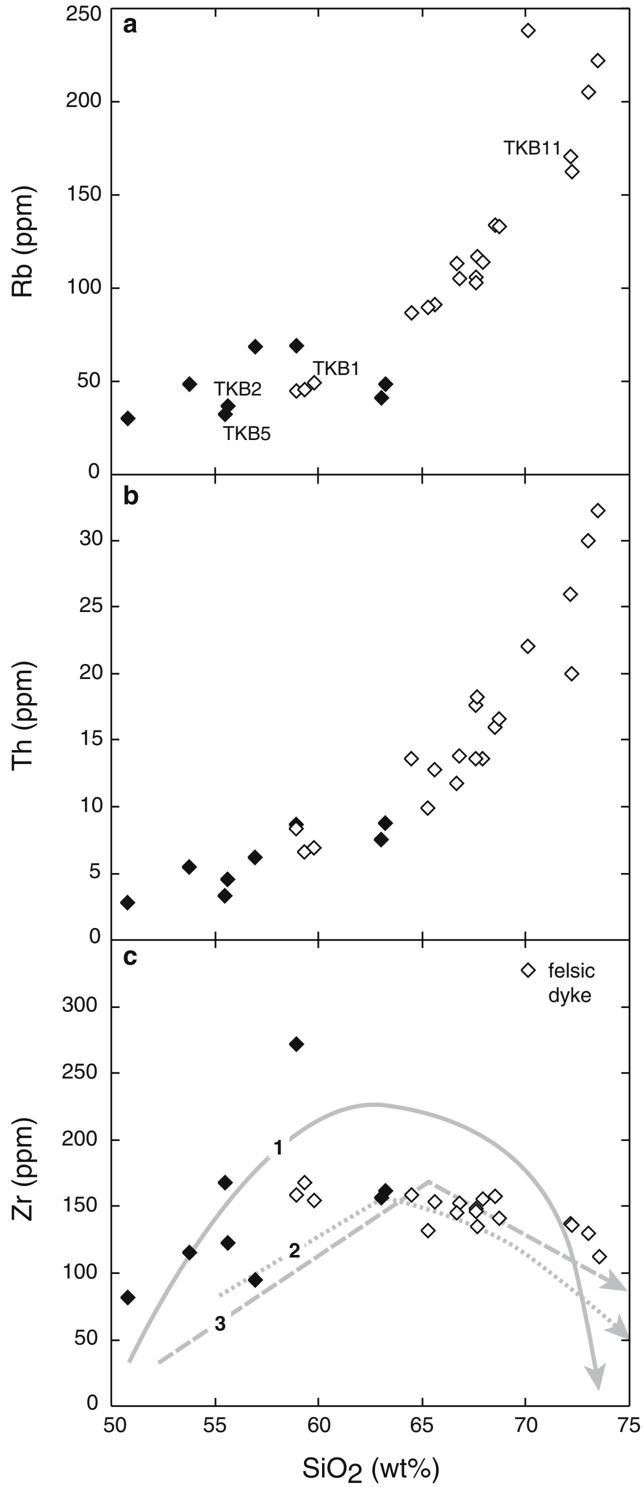

Fig. 9 Plots of **a** Rb, **b** Th and **c** Zr against silica for granitic rocks of the Cobargo Suite (*open symbols*) and the spatially associated dioritic-gabbroic rocks and enclaves contained by the granites (*filled symbols*). Note that in (**c**) the Zr-rich felsic dyke plots at the high silica extension of the array defined by the mafic (accumulative) rocks. The broad trends defined by (1) Loch Doon (Tindle and Pearce 1981), (2) Tuolumne (Bateman and Chappell 1979) and (3) the Boggy Plain (Hoskin 2000) intrusions are shown in (**c**) for comparison

Formation of the Cobargo Suite

Two end-member scenarios can be visualised for magma chamber crystallisation. The first, termed 'convective fractionation' (Rice 1981; Langmuir 1989; see Wyborn et al. 2001), is where crystallisation is driven by heat loss at the pluton margins, such that a solidification front slowly propagates inwards though the cooling pluton. Liquidus minerals are efficiently accreted at the pluton sidewalls, whereas the buoyant, differentiated melt escapes the crystallisation zone to either form a separate reservoir at the top of the magma chamber or erupts at the surface. Some residual liquid also back-mixes into the interior of the intrusion, driving the aphyric parental magma towards more evolved compositions. This mechanism pertains to hot, rather dry liquids that ascend to shallow or subvolcanic crustal levels, and can form vertically stratified and laterally zoned plutons associated with crystal-poor rhyolites. The Boggy Plain pluton is an example (Wyborn et al. 2001), as is the Palisade Crest Suite of the Sierra Nevada Batholith (Sawka et al. 1990) and the two-pyroxene Loch Doon pluton, Scotland (Tindle and Pearce 1981). The second situation is where crystallisation is promoted by undercooling in response to degassing of slightly cooler, volatile-charged magmas (e.g. Cashman and Blundy 2000). This can occur at greater crustal depths, and en route to the emplacement site in magma conduits. Nucleation and crystal growth throughout the magma volume results in solidification on rapid timescales that preclude melt-crystal segregation, and so relatively homogenous plutons result. This process could explain the formation of large, unzoned tonalites in subduction-related settings, such as those of the American Cordillera.

The evolution of the Cobargo Suite may have involved both processes, reflecting intermediate water contents (Fig. 10). Solidification of a zircon-undersaturated parental magma by crystallisation at the sidewalls and, to a lesser extent, in the pluton interior would lead to the formation of a broad 'mushy zone', with the complementary differentiated melt being displaced towards the centre and top of the pluton. The accumulative rocks are represented in part by satellite gabbros, some enclaves in the quartz diorite and the quartz diorite itself, and define the positive segment of the Zr-SiO_2 trend (Figs. 9c, 10). This reflects the concentration of incompatible Zr in the evolving melt, and its corresponding enrichment in the accumulating minerals and interstitial liquid (Wyborn et al. 2001).

Eventually, zircon saturation is attained within the mushy zone, so that the residual melt returned to the pluton interior drives the resident magma towards more felsic and Zr-poor compositions. Zircon crystallisation therefore initially occurs at temperatures far below those at the liquidus (~870°C), and from melts much more felsic than the bulk rock composition (~65% SiO_2, see below). As the density contrast between the differentiated melt and bulk magma decreases with crystallisation, greater amounts of the residual liquid will back-mix into the magma chamber, rather than migrate up the pluton walls (Wyborn et al. 2001). However, the proportion of residual melt that is retained in the crystallisation zone should also increase as the pluton solidifies inwards, since increasing viscosity and accelerated crystallisation impedes segregation of melt and crystalline phases. The rocks that define the negative Zr-SiO_2 trend on Fig. 10 therefore comprise different proportions of accumulated crystallising minerals and trapped, variably evolved melt, such that the composition of the most felsic samples converges towards that of the bulk magma. The moderate decrease in Zr compared to a much stronger rise in silica reflects the inefficient separation of zircons from the viscous melt in the crystallisation zone. This causes the increase in T_{Zr} shown by the Cobargo Suite, since in this case the decreasing T_{Zr} induced by the falling melt Zr content is exceeded by the opposite effect of silica in enhancing the thermal stability of zircon.

Sidewall crystallisation explains the localisation of the quartz diorite at the periphery of the relatively felsic Quaama Granodiorite, whereas the adjoining Coolagolite and Cobargo Granodiorites expose different levels through separate magma chambers. Many zoned plutons encompass a greater compositional range than does the Quaama Granodiorite, reflecting more protracted in situ crystallisation. The most mafic rocks of the latter are

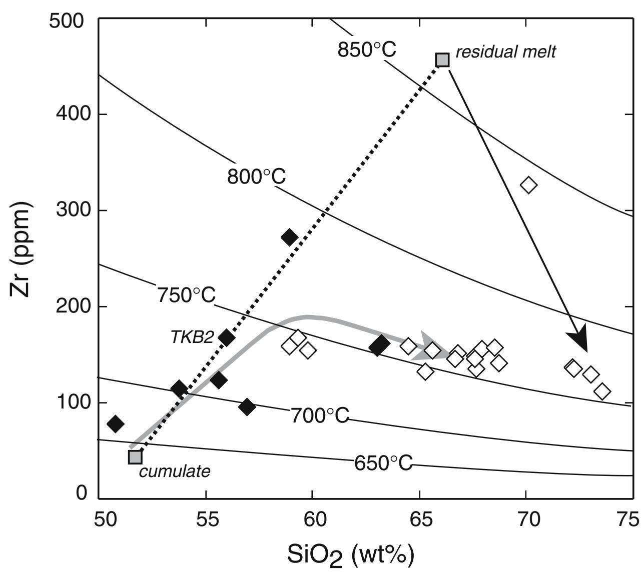

Fig. 10 Expanded Zr versus silica diagram for rocks of the Cobargo Suite, approximately contoured for T_{Zr}, showing the inferred evolution of zircon-saturated residual melts (*thin arrowed line*) and generalised trajectory of the accumulative magmas (*thick grey line*) during in situ crystallisation. The *dotted line* joins the estimated melt and solid components of diorite enclave TKB2. The contours plot the calculated Zr content of zircon-saturated melts as a function of silica and at a given temperature, according to the zircon solubility equation of Watson and Harrison (1983). The contours were derived using a general compositional relationship $M = -0.048SiO_2 + 4.65$ ($R^2 = 0.89$), which is defined by rocks of the Bega Batholith over the indicated silica range

Table 2 Estimation of zircon saturation temperature for diorite enclave TKB2

	Plagioclase	Cpx	Opx	It-Mt	Crystals	Bulk rock	Melt
SiO_2	52.5	52.8	51.5		51.7	56.1	66.1
TiO_2	0.2	0.3	0.3	46.0	0.8	0.9	1.0
Al_2O_3	29.5	2.5	1.7	1.1	17.4	16.8	15.4
FeO	0.5	8.3	22.9	51.0	7.8	6.8	4.4
MnO	0.01	0.27	0.4	1.0	0.17	0.13	0.04
MgO	1.1	14.6	20.7	1.5	8.3	6.7	2.8
CaO	9.9	19.6	1.5		10.1	7.7	2.3
Na2O	4.9	1.3	0.1		3.0	3.5	4.6
K_2O	0.4	0.1	0.1		0.3	1.1	2.9
P_2O_5	0.58	0.1	0.01		0.36	0.29	0.17
%	55	21	22	1.3	70		30
D_{Zr}	0.01	0.45	0.05	2	0.1		
Zr ppm					44	168	457
T_{Zr} (°C)							869

The melt component (30%) and crystal assemblage (70%) were calculated on an anhydrous basis assuming that the cumulate crystals were 55% plagioclase, 21% clinopyroxene and 22% orthopyroxene (derived from the modes). The Zr content of the melt was derived using the appropriate partition coefficients quoted by Rollinson (1993), Ewart and Griffin (1994) and Forsythe et al. (1994). Mineral compositions are averages of electron microprobe data

not in situ but represented by diorite fragments derived from deeper levels in the magma chamber. These enclaves might have been eroded from the marginal crystal mush by upward displacement of less dense, more fluid magma, or during recharge by relatively primitive liquid, as evidenced by the intermingled microgranular enclaves. The hornfels xenoliths in the quartz diorite were probably entrained in the same fashion, or were stoped from the contact during the final emplacement of the pluton. Either way, the incorporation of hornfels enclaves into crystal mushes would restrict their assimilation and facilitate the survival of zircon xenocrysts. The single inherited zircon detected in the quartz diorite probably originated in this way.

Temperatures of the Cobargo Suite magmas

To deduce the thermal evolution of the Cobargo magmas, it is necessary to establish the proportion of crystals in the various rocks of the suite, accepting the inherent difficulties in this approach (e.g. Meurer and Boudreau 1998). The most felsic, phenocryst-poor microgranites approximate zircon-saturated melts, so that T_{Zr} of these rocks is a reasonable proxy for the magmatic temperature at the final stages of differentiation. Considering the lower silica rocks, the diorite enclave TKB2 has the highest Zr content, and its position near the inflection on the Zr-SiO_2 trend suggests that it was formed from a magma that was approaching zircon saturation. However, T_{Zr} is unrealistically low (718°C) for this sample, because the bulk rock Zr is not a true measure of the actual Zr content of the melt when zircon saturation was attained.

The minimum amount of melt in TKB2 is approximated by the modes of interstitial quartz, biotite and amphibole (~20%). However, the finer matrix of this rock constitutes 30–35%, and this is probably a more realistic estimate of the crystallised liquid fraction. Taking a melt fraction of 30%, from a bulk rock Zr content of 168 ppm, and using a bulk D_{Zr} of 0.1, yields a melt Zr content of ~460 ppm (Table 2). Given the cumulus mineral assemblage, mass balance calculations require that the melt was significantly more felsic than the bulk rock, resembling a calc-alkaline dacite with 66% SiO_2 (Table 2). A melt of this composition is in equilibrium with zircon at ~870°C (Fig. 10). This represents the temperature of the highly crystalline diorite magma upon zircon saturation, and thus the onset of zircon crystallisation within the magma chamber. Some of the high-Zr felsic dykes that crosscut the Cobargo plutons may be segregated residual melts, perhaps expelled from the underlying cumulate pile during compaction (e.g. Sparks et al. 1985). The discrepancy between the temperature of the dioritic magma inferred by this approach and the T_{Zr} calculated from the bulk rock composition reflects the precipitated (cumulate) crystal content of the magma upon zircon saturation. Only by isolating the melt component can zircon saturation temperatures in crystal-rich magmas be properly estimated.

Conclusions

This study highlights the petrogenetic information that can be obtained by linking zircon U-Pb micro-geochronology with bulk rock geochemistry and zircon saturation thermometry. Specifically, the patterns of Zr-SiO_2 and T_{Zr}-SiO_2 for three metaluminous tonalite suites reveal a pivotal role for fractional crystallisation, although the exact scenario differed in each case. The pre-magmatic zircons in the 415 Ma Jindabyne Suite and 400 Ma Why Worry Suite appear to have been derived from metasedimentary rock, or magmas sourced therefrom, rather than from a meta-igneous protolith. In the Why Worry Suite, these grains were entrained into crystal-charged magmas that were precipitating zircon at temperatures well below the liquidus, whereas the inherited cores in the Jindabyne Suite were metastably preserved in hotter, more fluid magmas. The older zircons therefore monitor the input of an evolved supracrustal component in metaluminous granitic magmas, which should be clarified by detailed isotopic studies.

The clearest petrogenetic insight is gained from plutons of the 390 Ma Cobargo Suite, whose virtual lack of inherited zircon reflects magma generation at temperatures in excess of zircon stability. The negative Zr-SiO_2 trend requires subsequent zircon separation, though low T_{Zr} argues against the precipitation of zircon at the liquidus. These features are explicable by the crystallisation of a zircon-undersaturated ancestral magma, such that the mafic rocks are cumulates and the 'granitic' rocks solidified from suspensions of melt-precipitated minerals and residual, zircon-saturated melt, the proportion of the latter increasing in the more felsic rocks. The onset of zircon crystallisation in the magma chamber was delayed until the residual melt reached 65% SiO_2 and 460 ppm, at ~870°C. Such models offer an alternative explanation for the geochemical variation defined by the LFB granites that overcome the difficulties with explaining these trends by binary magma mixing or restite unmixing (Collins 1998), or with the granites forming via conventional liquid lines of descent (Chappell 1996). Most of the mafic cumulates for the Cobargo Suite are located at depth, reflecting the earlier onset of crystallisation of relatively hydrous magmas compared to hot, dry melts that formed the Boggy Plain pluton. Generation of silicic melts by crystallisation of water-rich magmas ponded in the deep crust has recently been proposed for the Izu-Bonin (Tamura and Tasumi 2002), Aeolian (Santorini: Mortazavi and Sparks 2004) and Costa Rican arcs (Vogel et al. 2004) and explains the paucity of mafic or cumulate plutons at the exposure level of the LFB. Fluid efflux from stalled and crystallising 'wet' magmas will induce melting of any juxtaposed metasedimentary wall-rocks, from where older zircons can be readily entrained. This situation may partly account for the evolved isotope ratios of inheritance-rich hornblende tonalites, like those of the Why Worry Suite.

In summary, the presence of inherited zircons and low T_{Zr} are unreliable indices of initial magma temperature. The nature of the inheritance must be carefully assessed in tandem with zircon morphology and whole-rock chemical trends before the 'low temperature' designation and its petrogenetic implications are valid. Low T_{Zr} in hornblende tonalites probably reflects initial zircon undersaturation, where zircon precipitation eventually occurred within a magma that had experienced prior crystallisation. Nonetheless, unravelling the patterns of Zr and T_{Zr} variations allows valuable deductions about the temperatures and crystallinity of granitic magmas, constraining models for their generation.

Acknowledgements This work is part of TK's Natural Environment Research Council postdoctoral fellowship (NER/I/S/2000/00942). Ion microprobe analysis at NRM through the High Lat resource was supported by the European Community-funded fifth framework programme 'Improving Human Potential'. The ion microprobe facility is operated under an agreement between the Nordic Research Councils, the Geological Survey of Finland and the Swedish Museum of Natural History. TK would like to thank Professor Y. Hiroi and the organisers of the 2003 Hutton V meeting in Toyohashi, Japan, where an earlier form of this work was presented. Astute and thought-provoking journal reviews by J. M. Palin (who suggested the T_{Zr} contouring as shown in Fig. 10), Calvin Miller and Bill Collins are gratefully acknowledged, as are discussions with Steve Sparks, Jon Blundy, Bruce Chappell, Ian Williams and Bruce Paterson about the aspects of this work. This is Nordsim contribution 114.

References

Amelin Y (1998) Geochronology of the Jack Hills detrital zircons by precise U-Pb isotope dilution analysis of crystal fragments. Chem Geol 146:25–38

Bacon CR (1986) Magmatic inclusions in silicic and intermediate volcanic rocks. J Geophys Res 91:6091–6112

Bateman PC, Chappell BW (1979) Crystallisation, fractionation and solidification of the Tuolumne Intrusive series, Yosemite National Park, California. Geol Soc Am Bull 90:465–482

Bea F (1996) Controls on the trace element composition of crustal melts. Trans Roy Soc Edinb Earth Sci 87:33–41

Bea F, Fershtater G, Corretgé LG (1992) The geochemistry of phosphorus in granitic rocks and the effect of aluminium. Lithos 29:43–56

Black LP, Kamo S, Allen CM, Davis DW, Aleinikoff JN, Valley JW, Mundil R, Campbell IH, Korsch R, Williams IS, Foudoulis C (2004) Improved $^{206}Pb/^{238}U$ ion microprobe geochronology by the monitoring of a trace element-related matrix effect; SHRIMP, ID-TIMS, ELA-ICP-MS and oxygen isotope documentation for a series of zircon standards. Chem Geol 205:115–140

Blundy JD, Sparks RSJ (1992) Petrogenesis of mafic inclusions in granitoids of the Adamello Massif, Italy. J Petrol 33:1039–1104

Burnham CW (1992) Calculated melt and restite contents of some Australian granites. Trans Roy Soc Edinb Earth Sci 83:387–398

Cashman K, Blundy JD (2000) Degassing and crystallisation of ascending andesite and dacite. Philos Trans R Soc Lond A358:1487–1513

Chappell BW (1996) Compositional variation within granite suites of the Lachlan Fold Belt: its causes and implications for the physical state of granitic magma. Trans Roy Soc Edinb Earth Sci 88:159–170

Chappell BW, Stephens WE (1988) Origin of infracrustal (I-type) granite magmas. Trans Roy Soc Edinb Earth Sci 79:71–86

Chappell BW, White AJR (1974) Two contrasting granite types. Pac Geol 8:173–174

Chappell BW, White AJR, Wyborn D (1987) The importance of residual source material (restite) in granite petrogenesis. J Petrol 28:1111–1138

Chappell BW, White AJR, Williams IS (1991) A transverse section through granites of the Lachlan Fold Belt. In: Second hutton symposium excursion guide. Bureau of Mineral Resources, Canberra

Chappell BW, Bryant CJ, Wyborn D, White AJR, Williams IS (1998) High- and low-temperature I-type granites. Res Geol 48:225–236

Chappell BW, White AJR, Williams IS, Wyborn D, Hergt JM, Woodhead JD (1999) Discussion: evaluation of petrogenetic models for Lachlan Fold Belt granitoids: implications for crustal architecture and tectonic models. Aust J Earth Sci 46:827–831

Chappell BW, White AJR, Williams IS, Wyborn D, Wyborn LAI (2000) Lachlan Fold Belt granites revisited: high- and low-temperature granites and their implications. Aust J Earth Sci 47:123–138

Chen Y, Williams IS (1990) Zircon inheritance in mafic inclusions from Bega Batholith granites, southeastern Australia: An ion microprobe study. J Geophys Res 95:17787–17796

Clemens JD (2003) S-type granites-models and evidence. Earth Sci Rev 61:1–18

Collins WJ (1998) Evaluation of petrogenetic models for Lachlan Fold Belt granitoids: implications for crustal architecture and tectonic models. Aust J Earth Sci 45:483–500

Collins WJ (1999) Reply: evaluation of petrogenetic models for Lachlan Fold Belt granitoids: implications for crustal architecture and tectonic models. Aust J Earth Sci 46:831–836

Collins WJ, Richards SR, Healy B, Ellison PI (2000a) Granite magma transfer, pluton construction, the role of mafic magmas and the metamorphic response: southeastern Lachlan Fold Belt, Australia. Geol Soc Aust Spec Publ FP3: 142pp

Collins WJ, Richards SR, Healy B, Wiebe RA (2000b) Origin of heterogeneous mafic enclaves by two-stage hybridisation in magma conduits (dykes) below and in granite magma chambers. Trans Roy Soc Edinb Earth Sci 891:27–46

Corfu F, Hanchar JM, Hoskin PWO, Kinny P (2003) Atlas of zircon textures. In: Hanchar JM, Hoskin PWO (eds) Zircon. Rev Mineral Geochem 53:468–500

Elburg MA (1996) U-Pb ages and morphologies of zircon in microgranitoid enclaves and peraluminous host granite: evidence for magma mingling. Contrib Mineral Petrol 123:177–189

Ewart A, Griffin WL (1994) Application of proton-microprobe data to trace element partitioning in volcanic rocks. Chem Geol 117:251–284

Forsythe LM, Nielsen RL, Fisk MR (1994) High field strength element partitioning between clinopyroxene and basaltic to dacitic magmas. Chem Geol 117:107–125

Gray CM (1984) An isotopic mixing model for the origin of granitic rocks in southeastern Australia. Earth Planet Sci Lett 70:47–60

Gray DR (1997) Tectonics of the southeastern Australian Lachlan Fold Belt: structural and thermal aspects. In: Burg J-P, Ford M (eds) Orogeny through time. Geol Soc Spec Publ 121:149–177

Gray DR, Foster DA (1997) Orogenic concepts—application and definition: Lachlan Fold Belt, eastern Australia. Am J Sci 297:859–891

Hine R, Williams IS, Chappell BW, White AJR (1978) Contrasts between I- and S-type granitoids of the Kosciuszko Batholith. J Geol Soc Aust 25:219–234

Hoskin PWO (2000) Patterns of chaos: fractal statistics and the oscillatory chemistry of zircon. Geochim Cosmochim Acta 64:1905–1923

Hoskin PWO, Kinny PD, Wyborn D, BW Chappell (2000) Identifying accessory mineral saturation during differentiation in granitoid magmas: an integrated approach. J Petrol 41:1365–1396

Huang WL, Wyllie PJ (1986) Phase relationships of gabbro-tonalite-granite-water at 15 kbar with applications to differentiation and anatexis. Am Mineral 71:301–316

Keay S, Collins WJ, McCulloch MT (1997) A three component Sr-Nd isotopic mixing model for granitoid genesis, Lachlan Fold Belt, eastern Australia. Geology 25:307–310

Keay S, Steele D, Compston W (1999) Identifying granite sources by SHRIMP U-Pb zircon geochronology: an application to the Lachlan Fold Belt. Contrib Mineral Petrol 137:323–341

Kemp AIS (2004) Petrology of high-Mg igneous rocks of the Glenelg River Complex, southeastern Australia, and the nature of their interaction with crustal melts. Lithos 78:119–156

Kemp AIS, Hawkesworth CJ (2003) Granitic perspectives on the generation and secular evolution of the continental crust. In: Treatise of geochemistry, vol 12. The Crust, Elsevier Science, Oxford, pp 349–410

Langmuir CH (1989) Geochemical consequences of in situ crystallisation. Nature 340:199–205

Lewis PC, Glen RA, Pratt GW, Clarke I (1994) Bega-Mallacoota 1:250 000 Geological Sheet SJ/55–4. Explanatory notes. Geol Surv NSW, Sydney, p 148

Ludwig KR (2001) Isoplot/Ex rev. 2.49. Berkeley Geochronology Centre, Spec Pub1a

Maas R, Nicholls IA, Greig A, Nemchin S (2001) U-Pb zircon studies of mid-crustal metasedimentary enclaves from the S-type Deddick Granodiorite, Lachlan Fold Belt, SE Australia. J Petrol 42:1429–1448

McCulloch MT, Chappell BW (1982) Nd isotopic characteristics of S- and I-type granites. Earth Planet Sci Lett 58:51–64

Meurer WP, Boudreau AE (1998) Compaction of igneous cumulates, Part 1: geochemical consequences for cumulates and liquid fractionation trends. J Geol 106:281–292

Miller CF, McDowell SM, Mapes RW (2003) Hot and cold granites? Implications of zircon saturation temperatures and preservation of inheritance. Geology 31:529–532

Mortazavi M, Sparks RSJ (2004) Origin of rhyolite and rhyodacite lavas and associated mafic inclusions of Cape Akrotiri, Santorini: the role of wet basalt in generating calc-alkaline silicic magmas. Contrib Mineral Petrol 146:397–413

Patiño Douce AE, Harris N (1998) Experimental constraints on Himalayan anatexis. J Petrol 39:689–710

Petford N, Gallagher K (2001) Partial melting of mafic (amphibolitic) lower crust by periodic influx of basaltic magma. Earth Planet Sci Lett 193:483–499

Piwinski AJ, Wyllie PJ (1968) Experimental studies of igneous rock series: a zoned pluton in the Wallowa Batholith, Oregon. J Geol 76:205–234

Pupin JP (1980) Zircon and granite typology. Contrib Mineral Petrol 73:207–220

Rice A (1981) Convective fractionation: a mechanism to provide cryptic zoning (macrosegregation), layered cresscumulates, banded tuffs and explosive volcanism in igneous processes. J Geophys Res 86:405–417

Rollinson H (1993) Using geochemical data: evaluation, presentation, interpretation. Longman Scientific and Technical, Essex

Sawka WN (1988) REE and trace element variations in accessory minerals and hornblende from the strongly zoned McMurry Meadows Pluton, California. Trans Roy Soc Edinb Earth Sci 79:157–168

Sawka WN, Chappell BW, Kistler RW (1990) Granitoid compositional zoning by side-wall boundary layer differentiation: evidence from the Palisade Crest Intrusive Suite, Central Sierra Nevada, California. J Petrol 31:519–553

Sparks RSJ, Huppert HE, Kerr RC, McKenzie DP, Tait SR (1985) Post-cumulus processes in layered intrusions. Geol Mag 122:555–568

Stacey JS, Kramers JD (1975) Approximation of terrestrial lead isotope evolution by a two stage model. Earth Planet Sci Lett 26:207–221

Stern CR, Huang WL, Wyllie PJ (1975) Basalt-andesite-rhyolite-H_2O: crystallisation interval with excess H_2O and H_2O-undersaturated liquidus surfaces to 35 kilobars, with implications for magma genesis. Earth Planet Sci Lett 28:189–196

Tamura Y, Tasumi Y (2002) Remelting of an andesitic crust as a possible origin for rhyolitic magma in oceanic arcs: an example from the Izu-Bonin arc. J Petrol 43:1029–1047

Tindle AG, Pearce JA (1981) Petrogenetic modelling of in situ fractional crystallisation in the zoned Loch Doon pluton, Scotland. Contrib Mineral Petrol 78:196–207

Vavra G (1990) On the kinematics of zircon growth and its petrogenetic significance. Contrib Mineral Petrol 106:90–99

Veevers JJ (2000) Antarctic Beardmore - Ross and Mirny Provenances saturate Paleozoic-Mesozoic east Gondwanaland with 0.6–0.5 Ga zircons. In: Veevers JJ (ed) Billion-year earth history of Australia and neighbours in Gondwanaland. Gemoc Press, Sydney

Vernon RH (1983) Restite, xenoliths and microgranitoid enclaves in granites. J Proc Roy Soc NSW 116:77–103

Vernon RH (1984) Microgranitoid enclaves: globules of hybrid magma quenched in a plutonic environment. Nature 304:438–439

Vernon RH (1990) Crystallisation and hybridism in microgranitoid enclave magmas: microstructural evidence. J Geophys Res 95:17849–17859

Vogel TA, Patino LC, Alvarado GE, Gans PB (2004) Silicic ignimbrites within the Costa Rican volcanic front: evidence for the formation of continental crust. Earth Planet Sci Lett 226:149–159

Wall VJ, Clemens JD, Clarke DB (1987) Models for granitoid evolution and source compositions. J Geol 95:731–749

Watson EB (1996) Dissolution, growth and survival of zircons during crustal fusion: kinetic principles, geological models and implications for isotopic inheritance. Trans Roy Soc Edinb Earth Sci 87:43–56

Watson EB, Harrison M (1983) Zircon saturation revisited: temperature and composition effects in a variety of crustal magma types. Earth Planet Sci Lett 64:295–304

Weidenbeck M, Alle P, Corfu F, Griffin WL, Meier M, Oberli F, von Quadt A, Roddick JC, Spiegel W (1995) Three natural zircon standards for U-Th-Pb, Lu-Hf, trace element and REE analysis. Geostand Newslett 19:1–23

White AJR, Chappell BW (1977) Ultrametamorphism and granitoid genesis. Tectonophys 43:7–22

Whitehouse MJ, Claesson S, Sunde T, Vestin J (1997) Ion microprobe U-Pb geochronology and correlation of Archaean gneisses from the Lewisian Complex of Gruinard Bay, north west Scotland. Geochim Cosmochim Acta 61:4429–4438

Whitehouse MJ, Kamber BS, Moorbath S (1999) Age significance of U-Th-Pb zircon data from early Archaean rocks of west Greenland—a reassessment based on combined ion microprobe and imaging studies. Chem Geol 160:201–224

Williams IS (1992) Some observations on the use of zircon U-Pb geochronology in the study of granitic rocks. Trans Roy Soc Edinb Earth Sci 83:447–458

Williams IS (2001) Response of detrital zircon and monazite, and their U-Pb isotopic systems, to regional metamorphism and host rock partial melting, Cooma Complex, southeastern Australia. Aust J Earth Sci 48:557–580

Williams IS, Chen YD, Chappell BW, Compston W (1988) Dating the source of the Bega Batholith granites by ion microprobe. Geol Soc Aust Abstr 21:424

Williams IS, Chappell BW, Chen YD, Crook KAW (1992) Inherited and detrital zircons—vital clues to the granite protoliths and early igneous history of southeastern Australia. Trans Roy Soc Edinb Earth Sci 83:503

Wyborn D, Chappell BW, James M (2001) Examples of convective fractionation in high temperature granites from the Lachlan Fold Belt. Aust J Earth Sci 48:531–542